Two long-axis dimensions of hippocampal cortical integration support memory function across the adult lifespan

Kristin Nordin[1,2,3], Robin Pedersen[3,4,5], Farshad Falahati[1,2], Jarkko Johansson[4,6], Filip Grill[7], Micael Andersson[4,5], Saana Korkki[1,2], Lars Bäckman[1,2], Andrew Zalesky[8,9], Anna Rieckmann[4,6,10], Lars Nyberg[4,5], Alireza Salami[1,2,3,4,5]

[1]Department of Neurobiology, Care Sciences, and Society, Karolinska Institutet, Solna, Sweden
[2]Aging Research Center, Karolinska Institutet and Stockholm University, Solna, Sweden
[3]Wallenberg Centre for Molecular Medicine, Umeå University, Umeå, Sweden
[4]Umeå Center for Functional Brain Imaging, Umeå University, Umeå, Sweden
[5]Department of Integrative Medical Biology, Umeå University, Umeå, Sweden
[6]Department of Radiation Sciences, Umeå University, Umeå, Sweden
[7]Donders Centre for Cognitive Neuroimaging, Radboud University, Nijmegen, the Netherlands
[8]Department of Biomedical Engineering, The University of Melbourne, Melbourne, VIC, Australia
[9]Department of Psychiatry, The University of Melbourne, Melbourne, VIC, Australia
[10]Department of Psychology, University of the Bundeswehr Munich, Germany

Ethics approval: This study was approved by the Regional Ethical board and the local Radiation Safety Committee in Umeå, Sweden.

Conflict of interest statement: The authors declare no conflict of interest.

Corresponding author: Kristin Nordin
Karolinska Institutet
Aging Research Center
Tomtebodavägen 18A
171 65 Solna, Sweden
E-mail: kristin.nordin@ki.se

Abstract

The hippocampus is a complex structure critically involved in numerous behavior-regulating systems. A multidimensional account of the hippocampus functional integration with neocortex, however, remains to be established and evaluated in terms of functional specialization and cognitive decline in aging. Here, we identify two long-axis modes of cortical functional connectivity (FC) during rest: a principal gradient of gradual anterior-posterior variation reflecting a task-positive/task-negative cortical motif, and a second-order gradient, representing unimodal-transmodal macroscale cortical organization. The second-order gradient predicted episodic memory and reflected underlying distribution of postsynaptic dopamine D1 receptors, suggesting shared principles of functional and neuromolecular organization. Older age was associated with less distinct transitions in FC along gradients, and a youth-like gradient profile, i.e. maintained distinctiveness, was linked to superior memory – highlighting age-related gradient dedifferentiation as a potential marker of cognitive decline. Our results support the notion that hippocampal function stands to inform general principles of brain organization, and emphasize a critical role of a second-order long-axis connectivity mode in mnemonic function across the lifespan.

Key words: Anteroposterior axis, Connectopic mapping, Dopamine, Episodic memory, Gradient mapping

The hippocampus plays a critical role in human behavior beyond its well-established involvement in memory and spatial navigation (Burgess et al., 2002; Laurita & Spreng, 2017; Moscovitch et al., 2016; Nadel & Peterson, 2013; Squire, 2004). Contemporary views hold that its broad involvement in cognition emerges through the combination of its intrinsic circuitry and its widespread cortical connections – placing it at the interface of multiple behavioral systems (Eichenbaum, 2000; Moscovitch et al., 2016; Ranganath & Ritchey, 2012). Characterizing organizational principles of its integration with the larger cortical landscape is therefore key to our understanding of its contribution to cognition and to the many diseases associated with its dysfunction (Barnes et al., 2009; Braak & Braak, 1991; Campbell & MacQueen, 2004; P. J. Harrison, 2004; Lieberman et al., 2018; Xie et al., 2020).

Animal models (Amaral & Witter, 1989; Witter & Amaral, 2021), together with histological and functional descriptions in humans (Amunts et al., 2005; Kahn et al., 2008; Libby et al., 2012; Maass et al., 2015; Plachti et al., 2019), emphasize the hippocampus transverse and longitudinal (anteroposterior) axes in determining its functional organization. In humans, anteroposterior transitions in large-scale functional connectivity are informed by variation in microstructure (Adnan et al., 2016), gray matter covariance (Ge et al., 2019; Plachti et al., 2019), and gene expression (Vogel et al., 2020), and are widely considered shaping the hippocampus role in behavior (Grady, 2019; Persson et al., 2018; Poppenk et al., 2013), and its vulnerability to neurological disease (Lladó et al., 2018; Small et al., 2011). In cognitively healthy older adults, functional isolation of hippocampal regions from prefrontal areas and large-scale cortical networks has been described in association with their dysfunction during memory encoding and retrieval (Nyberg et al., 2019; Salami et al., 2014, 2016). Recent studies suggest that this disconnection could be driven by the spatial patterns in which Alzheimer's pathology accumulates (Berron et al., 2021; de Flores et al., 2022; T. M. Harrison et al., 2019). Investigating cortico-hippocampal interactions as determined by the hippocampus long-axis

might as such serve as an important tool in identifying early markers of cognitive decline in older age and preclinical dementia.

In parallel, driven by advances in neuroimaging data analysis, macroscale organization of neocortical function is increasingly understood in terms of overlapping topographic gradients reflecting distinct neurofunctional hierarchies (Huntenburg et al., 2018; Margulies et al., 2016; Shafiei et al., 2020). Recently, local representations of such neocortical modes have been demonstrated across transverse and longitudinal axes of the medial temporal lobe (MTL) (Paquola et al., 2020). Positioned at the top of the MTL hierarchy, throughout which the topography of cortical connectivity is largely preserved (Kahn et al., 2008; Libby et al., 2012; Maass et al., 2015; Witter & Amaral, 2021), the hippocampus, specifically, may also exhibit such local representations of behaviorally relevant cortical modes (Przeździk et al., 2019; vos de Wael et al., 2018). However, a comprehensive account of the hippocampus' position within this emerging framework of multidimensional macroscale brain organization remains to be established, and importantly, evaluated in terms of hippocampal functional specialization across the adult lifespan.

Gradient mapping studies in young adults describe a principal hippocampal gradient of cortical connectivity linking somatomotor and default-mode areas at one end, with occipital and frontoparietal areas at the other, on the basis of its longitudinal axis (Przeździk et al., 2019; Tian et al., 2020; vos de Wael et al., 2018). This hippocampal gradient may be interpreted as largely reflecting a macroscale dimension spanning task-negative and task-positive poles (Chase et al., 2015). Importantly, this principal long-axis gradient might function as a better predictor of memory compared to connectivity of discrete hippocampal parcels (Przeździk et al., 2019). While these observations extend current accounts, dominated by methods accentuating discrete borders along the hippocampus (Chase et al., 2015; Plachti et al., 2019; Poppenk & Moscovitch, 2011; Robinson et al., 2015; Zhong et al., 2019), they remain

restricted to young adults, and importantly, to overlapping samples of young participants (i.e. the Human Connectome Project: Van Essen et al., 2013).

Here, we investigate the multidimensional organization of hippocampal-cortical connectivity across the adult human lifespan using state-of-the-art gradient mapping methods, and map individual differences in gradient properties onto behavioral and molecular phenotypes. Dopamine (DA) is considered one of the most important modulators of hippocampus-dependent neurocognitive function (Edelmann & Lessmann, 2018; El-Ghundi et al., 2007). Animal models suggest heterogeneous innervation patterns by distinct DA sources (Gasbarri et al., 1994; Ishikawa et al., 1982; Kempadoo et al., 2016; Verney et al., 1985), as well as spatial variation in hippocampal postsynaptic DA receptors (Dubovyk & Manahan-Vaughan, 2019), across both transverse and longitudinal hippocampal axes, likely allowing for separation between DA modulation of distinct hippocampus-dependent behaviors (Edelmann & Lessmann, 2018). Relatedly, the human hippocampus has been suggested as part of distinct DA circuits on the basis of anteroposterior variation in its functional connectivity with midbrain and striatal regions (Kahn & Shohamy, 2013; Nordin et al., 2021; Nyberg et al., 2016). We therefore tested the hypotheses that the topography of hippocampal cortical connectivity might reflect the underlying distribution of postsynaptic DA D1 receptors (D1DRs).

We observed the hypothesized principal anteroposterior gradient, and in addition, a second-order mode of connectivity expressed along the hippocampal long-axis, separating communities of sensorimotor areas at one end from transmodal regions at the other. To elucidate the complimentary roles of these gradients for hippocampal functional specialization, we first characterized gradients by linking their cortical patterns to a) the macroscale layout of large-scale networks; b) meta-analytic functional activation in Neurosynth (Yarkoni et al., 2011); c) and tested individual differences in topographic properties of these gradients as predictors of episodic memory performance. Age-sensitivity of gradients was assessed across

the sample, and latent class analysis (LCA) (Vermunt & Magdison, 2002) identified older individuals exhibiting a youth-like gradient profile and superior memory function as distinct from age-matched older counterparts, suggesting a functional role of maintained hippocampal connectivity topography in older age.

Results

Multiple dimensions of hippocampal cortical integration across the adult lifespan

Connectopic mapping (Haak et al., 2018) was applied to resting-state fMRI data from 180 participants (90 men/90 women; 20-79 years; mean age = 49.8±17.4) from the DyNAMiC study (Nordin et al., 2022). As a replication data set, we used an independent sample of 224 adults (122 men/102 women; 29-85 years mean age = 65.0±13.0) from the Betula project (Nilsson et al., 2004; Nyberg et al., 2020). Connectopic mapping was used to extract the dominant modes of functional connectivity within the hippocampus based on non-linear manifold learning (Laplacian eigenmaps) applied to a similarity matrix derived from functional connectivity fingerprints computed between each hippocampal voxel and each voxel within neocortex. This identified a set of orthogonal connectopic maps (i.e. eigenvectors) describing overlapping connectivity topographies (i.e. gradients) within the hippocampus. Gradients were computed at subject level, and at group level across the sample, separately for the left and right hippocampus. We analyzed the first three gradients, together explaining 63% and 71% of the variance in left- and right-hemispheres, respectively. Furthermore, this number corresponded to a clear elbow in the scree plot (Supplementary Figure 1).

The principal gradient (G1), explaining 44% and 53% of the variance in left and right hemispheres, was organized along the hippocampus longitudinal axis, conveying gradual anterior-to-posterior variation in cortical connectivity (Figure 1A: c.f. Przeździk et al., 2019; Tian et al., 2020; vos de Wael et al., 2018). This pattern of connectivity change is illustrated by

dividing subject-level G1 connectopic maps into 23 long-axis bins of ~2mm and plotting the average gradient values as a function of their distance from the most anterior hippocampal voxel (Przeździk et al., 2019) (Figure 1B). The second-order gradient (G2), explaining 11% of the variance in both hemispheres, expressed a secondary long-axis gradient determined as organized from the middle hippocampus towards anterior and posterior ends (Figure 1A-B). Finally, the third-order gradient (G3: explaining 8 and 7% of the variance), reflected variation along the hippocampus transverse axis, such that inferior-lateral parts of the hippocampus were separated from medial-superior parts (Figure 1A-B). Inspecting G3 across sample-specific segmentations of cornu ammonis (CA1-3), dentate gyrus (DG/CA4), and subiculum subfields suggested that while CA1-3 reflected the full extent of the gradient, and DG/CA4 variation around its center, the subiculum reflected only the most inferior section of the gradient (Supplementary Figure 2). The three gradients were highly reproducible in the independent replication data set (Supplementary Figure 3). Correspondence between samples was determined by spatial correlations between gradient pairs (left hemisphere: G1: $r = 0.990$, $p < 0.001$; G2: $r = 0.946$, $p < 0.001$; G3: $r = 0.918$, $p < 0.001$; right hemisphere: G1: $r = 0.996$, $p < 0.001$; G2: $r = 0.969$, $p < 0.001$; G3: $r = 0.897$, $p < 0.001$).

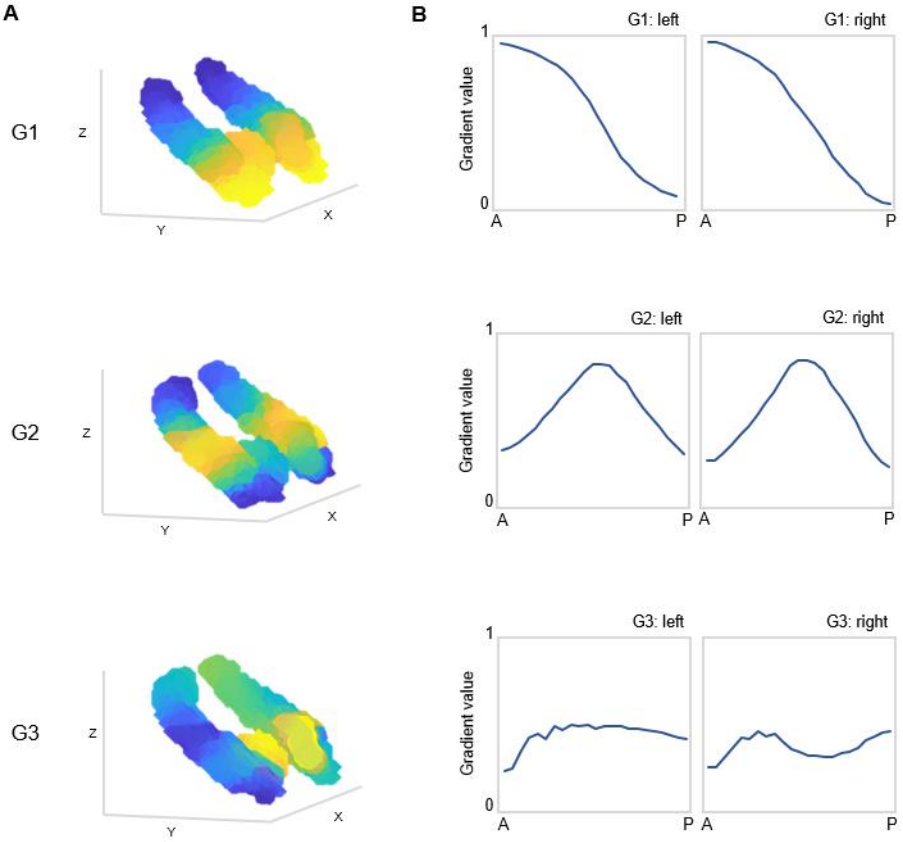

Figure 1. Topographic gradients of cortical connectivity within the hippocampus. A) The three first hippocampal connectopic maps (G1-G3), together explaining 67% of the variance across left and right hemispheres. Similar colors convey similar patterns of cortical connectivity. Values range between 0 (blue) and 1 (yellow). B) Plots convey change in connectivity along the anteroposterior hippocampal axis for the three gradients. For each gradient, mean values from 23 bins (each ~2mm) were plotted against their distance (in mm) from the most anterior hippocampal voxel. Values were estimated based on subject-level gradients and averaged across participants. G1 conveys gradual change in connectivity patterns along an anteroposterior gradient. G2 conveys gradual change in connectivity patterns along a second-order long-axis gradient, spreading from the middle hippocampus towards anterior and posterior ends. G3 conveys close to no change in connectivity along the hippocampus longitudinal axis, with connectivity change instead organized in a primarily medial-lateral gradient.

Hippocampal gradients reflect distinct dimensions of macroscale cortical organization

The projection of G1 onto cortex conveyed a pattern linking somatomotor and temporolimbic regions at the anterior end of the gradient with occipital and frontoparietal regions at the posterior end (Figure 2A). To further describe the cortical organization of G1, we examined the distribution of large-scale networks in gradient space by computing median gradient values for seven cortical networks (Yeo et al., 2011). This placed default-mode (left G1: 0.67; right G1: 0.61), limbic (left G1: 0.65; right G1: 0.63) and somatomotor (left G1: 0.67; right G1: 0.60) networks at anterior-to-middle parts of the gradient, whereas visual (left G1: 0.41; right G1: 0.52), frontoparietal (left G1: 0.29; right G1: 0.41) and ventral attention networks (left G1: 0.21; right G1: 0.12) toward the posterior end of the gradient (Figure 2B).

In contrast, G2 exhibited a unimodal-transmodal pattern across cortex. This pattern linked the middle hippocampus to medial frontal and posterior parietal regions, while anterior and posterior hippocampal ends to somatomotor and occipital regions (Figure 2A). Consistently, functional networks mapped onto G2 placing frontoparietal (left G2: 0.74; right G2: 0.82) and default-mode (left G2: 0.65; right G2: 0.74) networks at one end, while visual (left G2: 0.29; right G2: 0.12) and somatomotor networks (left G2: 0.17; right G2: 0.17) at the other end (Figure 2B). To further evaluate G2 as a local representation of the well-established unimodal-transmodal gradient of macroscale cortical organization (Margulies et al., 2016), we correlated cortical G2 values with values from a unimodal-transmodal cortical gradient previously reported in the DyNAMiC dataset (Pedersen et al., 2023). We observed positive correlations for G2 (left G2: Spearman's r = 0.29, p_{spin} = 0.062; right G2: Spearman's r = 0.43, p_{spin} = 0.002; Figure 2), greater than the non-significant correlations observed for G1 (left G1: Spearman's r = -0.03, p_{spin} = 0.578, Z = 4.59, p < 0.001; right G1: Spearman's r = 0.01, p_{spin} = 0.497, Z = 6.47, p < .001), and G3 (left G3: Spearman's r = -0.31, p_{spin} = 0.966, Z = 8.76, p < .001; right G3: Spearman's r = -0.40, p_{spin} = 0.983, Z = 12.49, p < 0.001; Figure 2C). Taken

together, we demonstrate different lines of converging evidence suggesting that G2 serves as a local map of the macroscale unimodal-transmodal axis of cortical organization.

The cortical projection of G3 primarily separated ventral attention areas from medial parietal and medial frontal areas. Aligning well with large-scale cortical connectivity profiles previously reported for hippocampal subfields (de Flores et al., 2017; Ezama et al., 2021; vos de Wael et al., 2018), we observed that areas of the default-mode network (left G3: 0.26; right G3: 0.17) most strongly mapped onto the most inferior end of G3, consistent with the reported connectivity profile of the subiculum, whereas ventral attention (left G3: 0.83; right G3: 0.75) and somatomotor (left G3: 0.54; right G1: 0.54) networks had a stronger medial position along G3, aligning with cortical connectivity reported for CA1-3 (Figure 2B).

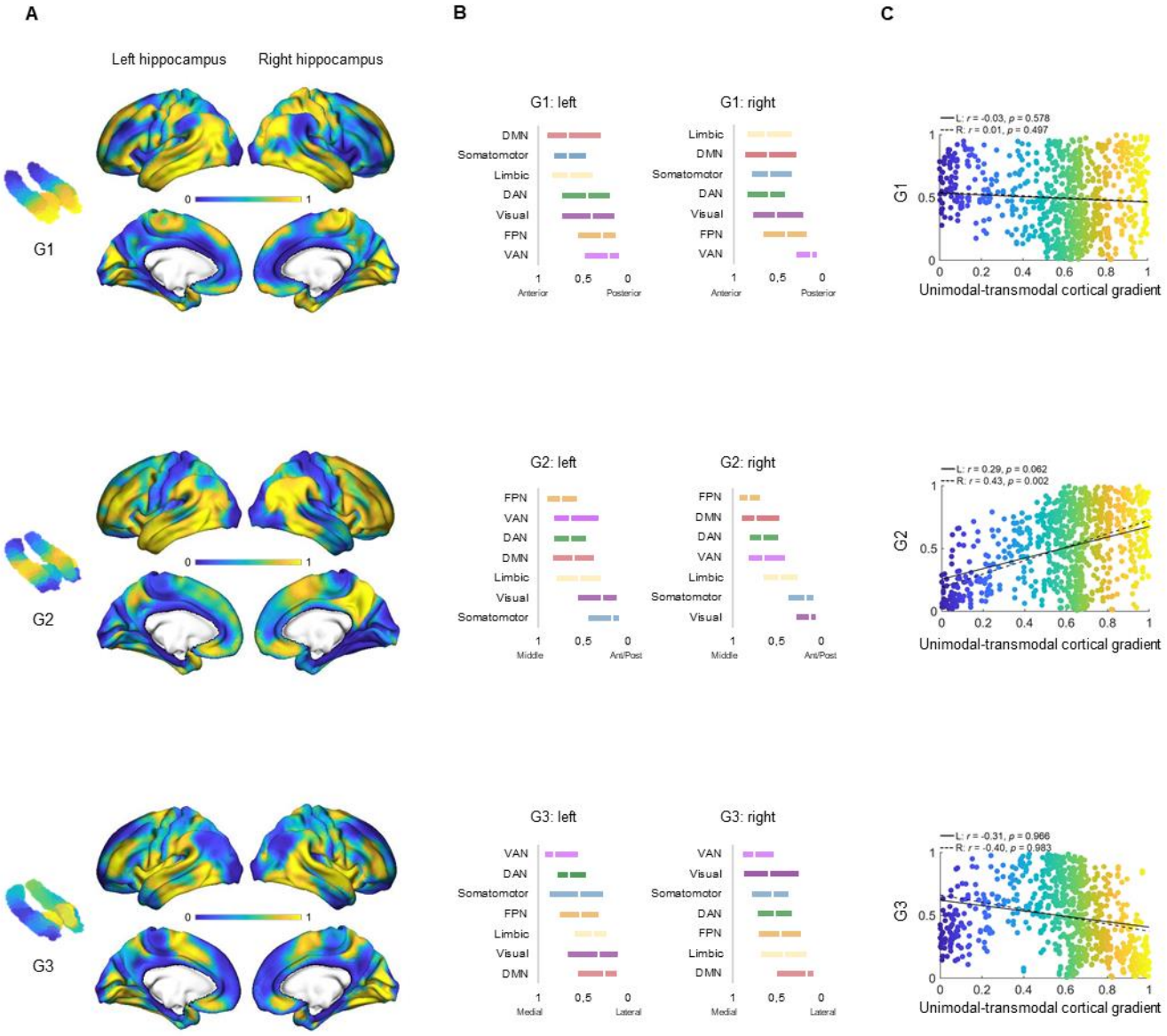

Figure 2. The cortical distribution of hippocampal gradients. A) Cortical projections for G1, G2, and G3. Values range between 0 (blue) and 1 (yellow). B) Distribution of cortical networks in gradient space. Bars represent 2nd and 3rd quartiles around median cortical gradient values within each of the seven networks in the Yeo 2011 parcellation (Yeo et al., 2011). C) Correlations between the cortical patterns of hippocampal gradients and a unimodal-transmodal cortical gradient previously reported in the DyNAMiC dataset by Pedersen et al., 2023.

Distinct patterns of behavioral transitions along G1 and G2

To further characterize the cortical integration conveyed by G1 and G2, and the relevance of these two modes of functional organization for hippocampal functional specialization, we mapped transitions in behavioral domains onto G1 and G2 using meta-analytical decoding in Neurosynth (Yarkoni et al., 2011). Correlations were assessed between meta-analytical maps of behavioral terms and twenty-percentile bins of each gradient's cortical projection (Figure 3). First, a selection of terms commonly linked to anteroposterior hippocampal functional specialization (Grady, 2019; Plachti et al., 2019) were assessed across G1 and ranked based on their location along the gradient (Figure 3A). This revealed an overarching verbal/social-to-spatial/cognitive axis. Terms that expressed the strongest anterior loadings on G1 included *words*, *social*, *recognition*, and *dementia*, whereas terms of *navigation*, *episodic memory*, *encoding* and *recollection* showed preferential posterior loadings. In contrast, behavioral transitions along G2 were expected to correspond to a perceptual/motor-associative axis, given its unimodal-transmodal organization (Figure 2A-C). Terms were selected and ordered based on a previous report demonstrating behavioral transitions along a unimodal-transmodal cortical axis (Margulies et al., 2016). This, indeed, separated *sensorimotor* and *visual* terms at one end from *social*, *self-referential*, and *default* terms at the other (Figure 3B), lending further support to the interpretation of G2 as a local representation of the unimodal-transmodal gradient of macroscale cortical organization.

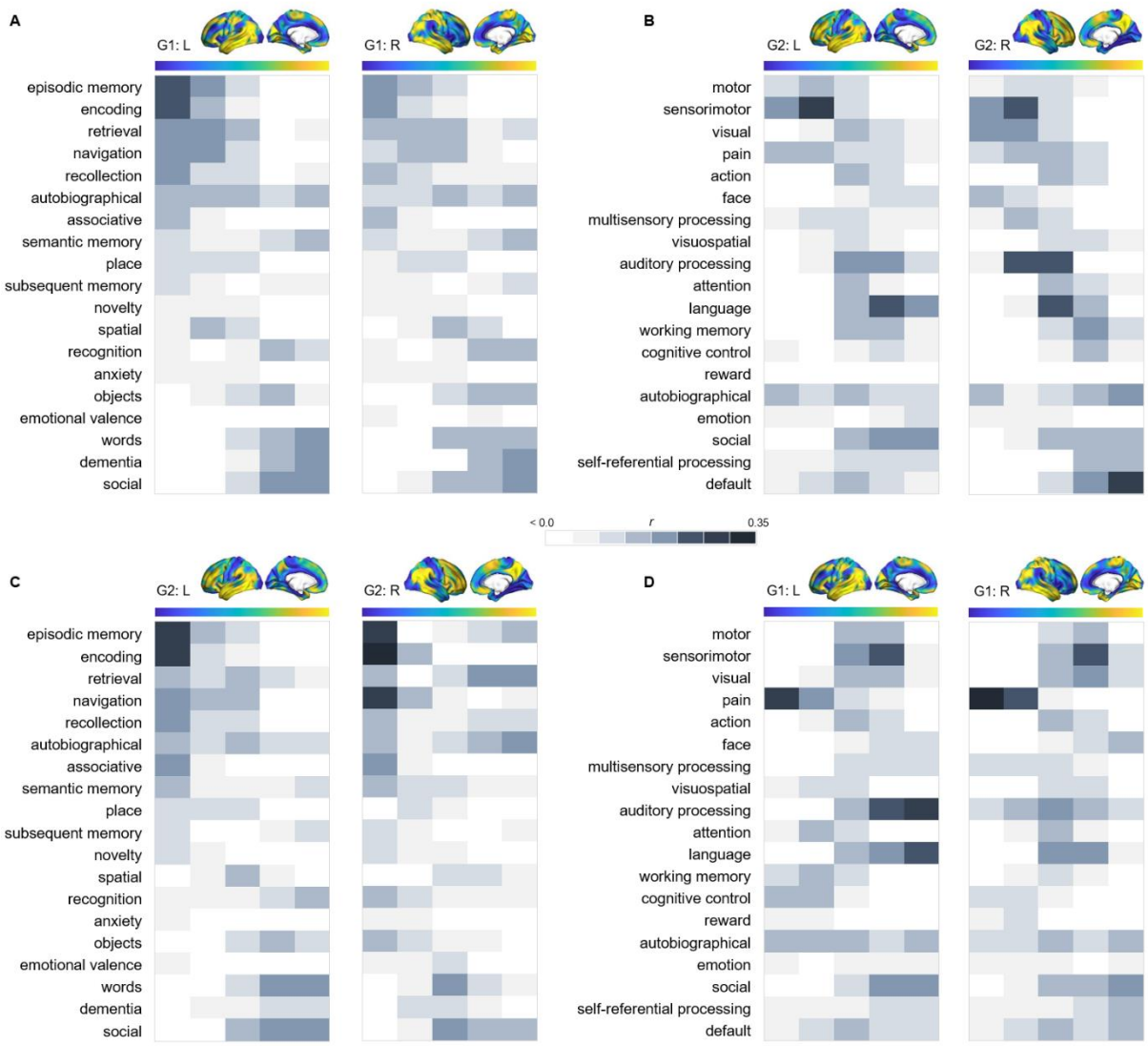

Figure 3. Behavioral profiling of G1 and G2. For each gradient, columns represents twenty-percentile bins of that gradient's cortical projection. Color shadings represent the strength of correlations between gradient bins and meta-analytical maps in Neurosynth. A) Terms commonly linked to anteroposterior hippocampal functional specialization were assessed across G1 and ranked based on their location along the gradient. This revealed an overarching verbal/social-to-spatial/cognitive axis, most evident across G1 in the left hemisphere. B) For G2, terms were selected and ordered based on a previous report demonstrating behavioral transitions along a unimodal-transmodal cortical axis (Margulies et al., 2016). C) The correspondence between G2 and behavioral terms commonly linked to anteroposterior hippocampal functional specialization. D) The correspondence between G1 and behavioral terms expressing a unimodal-transmodal axis.

Dedifferentiated gradient topography in older age

We next explored age-related differences in gradient topography. To this end, trend surface modelling (TSM) was applied to each subject-level connectopic map (Haak et al., 2018; Przeździk et al., 2019). This spatial statistics approach parameterizes gradients at subject level, yielding a set of spatial model parameters which describes the topographic characteristics of each gradient in x, y, z directions (Supplementary Figure 5). There was a significant effect of age on topographic characteristics of all three gradients, as assessed in a series of multivariate GLMs including age as the predictor and TSM parameters as dependent variables (controlling for sex and mean frame-wise displacement; FD). The principal gradient displayed the greatest effect of age (left: $F_{(9,150)} = 5.853$, $p < 0.001$, partial $\eta^2 = 0.260$; right: $F_{(9,150)} = 6.971$, $p < 0.001$, partial $\eta^2 = 0.298$), followed by G2 (left: $F_{(12,147)} = 2.583$, $p = 0.004$, partial $\eta^2 = 0.174$; right: $F_{(12,145)} = 2.635$, $p = 0.003$, partial $\eta^2 = 0.179$), and G3 (left: $F_{(12,147)} = 1.973$, $p = 0.030$, partial $\eta^2 = 0.139$; right: $F_{(12,145)} = 2.082$, $p = 0.021$, partial $\eta^2 = 0.147$). To visualize effects, subject-level gradient values were plotted along the anteroposterior axis, averaged within groups of young (20-39 years), middle-aged (40-59 years) and older (60-79 years) adults (Figure 4). Connectivity across the principal hippocampal gradient (G1) and secondary middle-to-anterior/posterior axis (G2) displayed less distinct differentiation at older age, depicted by the flatter curves in the older group. (Figure 4).

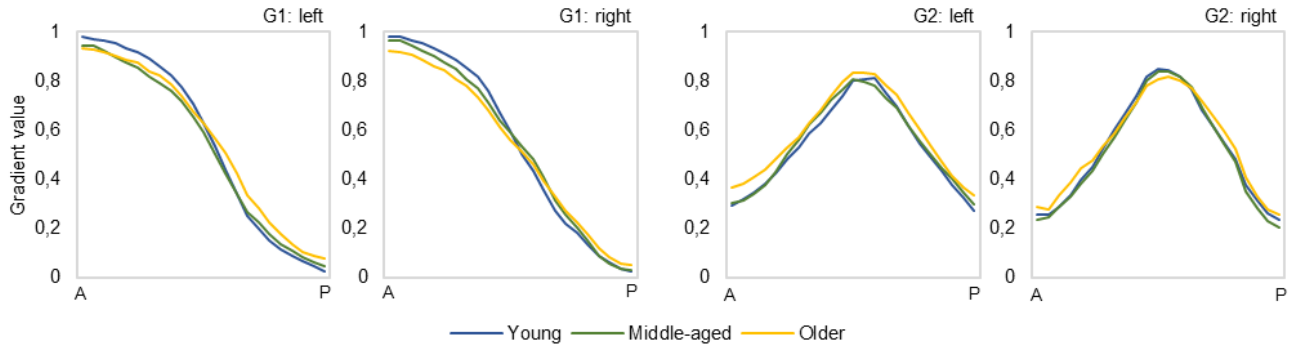

Figure 4. Less specificity in connectivity change across gradients in older age. Average values of subject-level G1 and G2 bins (~2mm) plotted as a function of their distance (in mm) from the most anterior hippocampal voxel. Separate lines are displayed for young (20-39 years; blue), middle-aged

(40-59 years, green), and older (60-79 years; yellow) age groups. The flatter curves in the older group indicate less distinct change in connectivity patterns across gradients in older age.

Topography of hippocampal gradients predicts episodic memory performance

Next, we investigated the relationship between individual differences in gradient topography and episodic memory. Using hierarchical multiple regression models, in which age, sex, and mean FD were controlled for in a first step (M1), we entered TSM parameters of the three gradients as predictors of episodic memory in a step-wise manner. Models were assessed separately for left and right hemispheres. Memory performance was, across the sample, significantly predicted by individual differences in G2 topography in the left hippocampus (Figure 5A), over and above covariates and topography of G1 (Adj. R^2 = 0.308, ΔR^2 = 0.096, F= 1.842, p = 0.047). Assessed within age groups, memory performance was in young adults predicted by left-hemisphere G1 topography (Adj. R^2 = 0.182, ΔR^2 = 0.357, F= 2.672, p = 0.015; Figure 5B). While these results converge with previous findings of left-hemisphere G1 topography predicting episodic memory performance in young adults (Przeździk et al., 2019), they highlight a critical contribution of G2 topography in explaining individual differences in episodic memory across the adult lifespan.

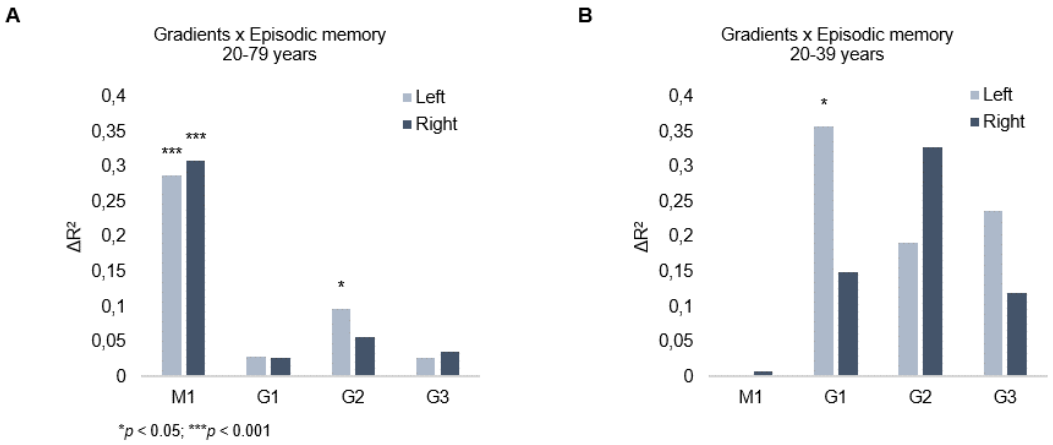

Figure 5. Hippocampal gradient topography as a predictor of episodic memory performance. A) Individual differences in topographic characteristics of G2 in the left hemisphere significantly predicted episodic memory performance across the sample, over and above the first- and second-step models (M1: age, sex, in-scanner motion; G1 parameters). B) Topographic characteristics of G1 in the left hemisphere

significantly predicted episodic memory performance in young adults, over and above M1 (age, sex, and in-scanner motion).

Topography of G2 reflects distribution of hippocampal dopamine D1 receptors

We have recently shown shared organizational principles between gradients of neocortical function and the DA D1 receptor (D1DR) (Pedersen et al., 2023). More specifically, we found that D1DR follow an associative-sensory axis of functional organization. On this view, it is perceivable that the local representation of the unimodal-transmodal cortical motif conveyed by our second-order functional gradient might be evident also in the distribution of hippocampal D1DRs. Individual maps of D1DR binding potential, estimated through [^{11}C]SCH23390 PET, were submitted to TSM yielding a set of spatial model parameters describing the topographic characteristics of hippocampal D1DR distribution for each participant. D1DR parameters were subsequently used as predictors of gradient parameters in a multivariate GLM (controlled for age, sex, and mean FD). D1DR topography significantly predicted topography of G2 (right hemisphere: $F = 1.207$, $p = 0.041$; partial $\eta 2 = 0.118$), but not for G1 (Figure 6). This association was evident across different D1DR TSM model orders (Supplementary Figure 5), suggesting shared principles of functional and neuromolecular organization within the hippocampus.

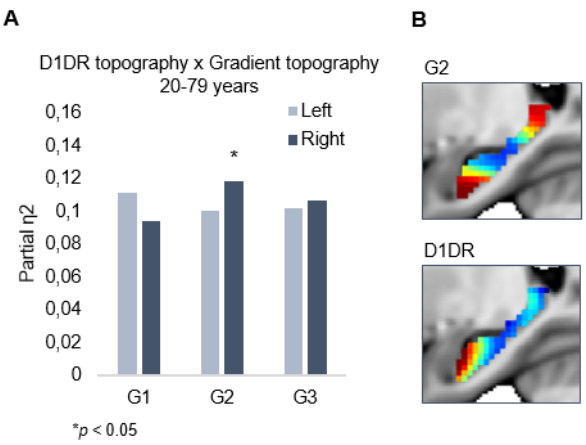

Figure 6. Topography of dopamine D1 receptor (D1DR) distribution as a predictor of gradient topography. A) Multivariate effects of hippocampal D1DR TSM parameters as predictors of G2 TSM parameters. B) Group-level G2 and hippocampal D1DR distribution in the right hemisphere. Note that the color scale of G2, which is arbitrary, has been flipped.

Youth-like gradient topography supports memory in older age

To investigate a functional role of the principal and most age-sensitive gradient in old age, we tested whether mnemonic functioning in older adults would be promoted by youth-like gradient topography. To identify distinct gradient profiles in older age, we applied data driven latent class analysis (LCA) to TSM parameters (residualized to account for age, sex, and mean FD) of left-hemisphere G1, which predicted episodic memory performance in younger adults. LCA yielded a two-class solution separating a smaller group (n=19) from a larger group (n=30) of older adults (60-79 years). By definition, these two groups differed in terms of left-hemisphere G1 characteristics ($F_{(9,37)} = 13.778$, $p < 0.001$, partial $\eta^2 = 0.770$), and a difference was also evident between groups in the right hemisphere ($F_{(9,37)} = 3.790$, $p = 0.002$, partial $\eta^2 = 0.480$).

Individuals in the smaller subgroup were determined as exhibiting an aged gradient profile, whereas older adults in the larger subgroup as exhibiting a youth-like gradient profile, given distinct patterns of differences in gradient parameters as compared to younger adults. Importantly, the classification based on G1 parameters extended across all three gradients in both hemispheres (Figure 7A), such that the smaller sub group displayed marked differences from younger adults across all gradients (left G1: $F_{(9,63)} = 15.549$, $p < 0.001$, partial $\eta^2 = 0.690$; right G1: $F_{(9,63)} = 5.322$, $p < 0.001$, partial $\eta^2 = 0.432$; left G2: $F_{(12,60)} = 3.991$, $p < 0.001$, partial $\eta^2 = 0.444$; right G2: $F_{(12,60)} = 2.192$, $p = 0.023$, partial $\eta^2 = 0.305$; left G3: $F_{(12,60)} = 2.832$, $p = 0.004$, partial $\eta^2 = 0.362$; right G3: $F_{(12,60)} = 1.844$, $p = 0.061$, partial $\eta^2 = 0.269$), while the youth-like sub group differed from young adults to a lesser extent in terms of G1 (left G1: $F_{(9,74)} = 4.416$, $p < 0.001$, partial $\eta^2 = 0.349$; right G1: $F_{(9,74)} = 3.086$, $p = 0.003$, partial $\eta^2 = 0.273$), and displayed second- and third-order gradients comparable to those in younger age (left G2: $F_{(12,71)} = 1.616$, $p = 0.107$, partial $\eta^2 = 0.215$; right G2: $F_{(12,71)} = 1.442$, $p = 0.168$, partial $\eta^2 = 0.196$; left G3: $F_{(12,71)} = 1.122$, $p = 0.357$, partial $\eta^2 = 0.159$; right G3: $F_{(12,71)} = 1.596$, $p = 0.112$, partial $\eta^2 = 0.212$). Examining change in connectivity along G1 and G2

demonstrated that the reduced topographic specificity observed across these two gradients in older age was driven by older adults with an aged gradient profile (Figure 7B). Both older sub groups, nevertheless, displayed altered gradient organization across cortex (Figure 7C-D). The distribution of cortical networks in G1 space indicated a shift towards a unimodal-transmodal organization in youth-like older adults, not evident in the aged older group (Figure 7D).

The two groups did not differ in terms of age (aged: 70.8±6.0; youth-like: 68.4±4.7; $t = 1.548$, $p = 0.128$), sex (aged: 9 men/10 women; youth-like: 16 men/14 women; $X^2 = 0.166$, $p = 0.684$), nor hippocampal gray matter (left hemisphere: aged: 4271.2±480.9; youth-like: 4246.8±269.1; $t = 0.223$, $p = 0.824$; right hemisphere: aged: 3866.2±446.3; youth-like: 3979.9±398.1; $t = 0.929$, $p = 0.357$). In line with our hypothesis, we observed superior memory in older adults exhibiting a youth-like gradient profile (Figure 7E): at trend-level for the composite episodic measure (aged: 43.2±3.7; youth-like: 46.5±6.6; $t = 1.958$, $p = 0.056$), driven by a significant group difference on its word recall sub test (aged: 40.9±4.5; youth-like: 43.4±6.8; $t = 2.600$, $p = 0.012$). Word recall performance was furthermore predicted by left-hemisphere G1 parameters (over and above age, sex, and mean FD) in the youth-like older adults (Adj. $R^2 = 0.464$, $\Delta R^2 = 0.543$, $F = 3.043$, $p = 0.028$), while no such association was observed in the aged sub group (Adj. $R^2 = 0.063$, $\Delta R^2 = 0.533$, $F = 1.004$, $p = 0.518$).

Classification of older adults based on right-hemisphere G1 TSM parameters is presented in the Supplementary Information. While this also yielded a two-class solution, the resulting groups primarily differed in terms of right-hemisphere G1 parameters (Supplementary Figure 6), with group differences less pronounced for subsequent gradients. This indicates that topography of G1 in the left-hemisphere, predictive of episodic memory in young adults, does a better job at informing comprehensive youth-like and aged gradient profiles in older age. Taken together, our results suggest that maintaining youth-like organization of hippocampal function is concomitant with more efficient mnemonic function in older age.

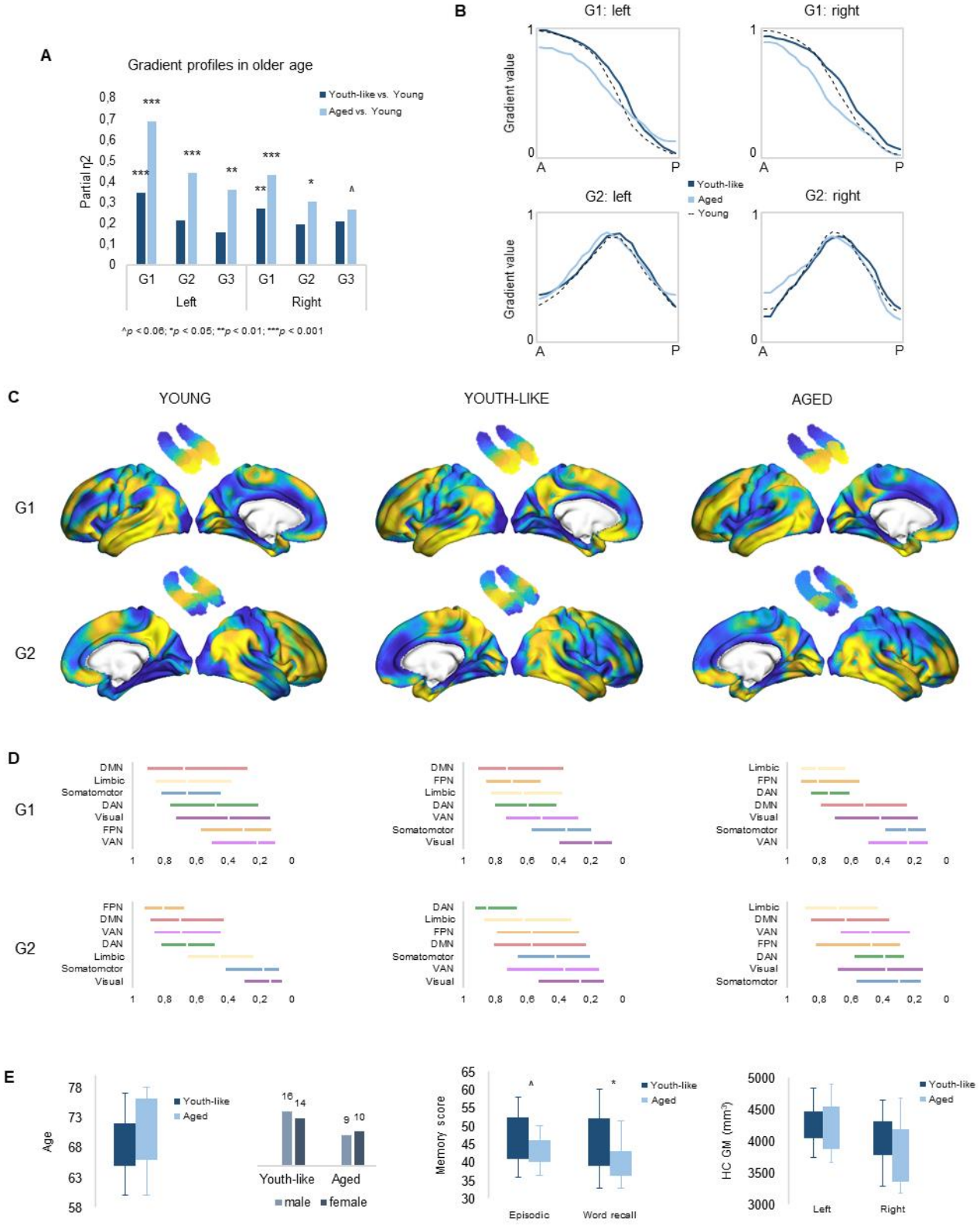

Figure 7. Gradient profiles in older age. A) Two groups of older adults were identified based on left-hemisphere G1 parameters. The first group (n=19) displayed gradient characteristics significantly different from those in young adults, whereas the second group (n=30) displayed gradient characteristics more similar to those in young adults. Bars represent comparisons of gradient TSM parameters between

older sub groups and younger adults. B) Average gradient values across participants within sub groups, plotted against the distance (in mm) from the most anterior hippocampal voxel. The flatter curves in older adults with an aged gradient profile suggest less distinct change in connectivity across hippocampal gradients. C) Group-level G1 and G2 for young, youth-like, and aged groups. D) Distribution of cortical networks in gradient space. E) Older sub groups were comparable in terms of age, sex, and hippocampal gray matter (GM) volume, while older adults with a youth-like gradient profile exhibited greater episodic memory function.

Discussion

Here, we provide, for the first time, a multidimensional characterization of functional hippocampal cortical integration across the adult human lifespan, and map topography of connectivity gradients onto behavioral phenotypes. Specifically, our results emphasize two functional modes organized along the hippocampus longitudinal axis in understanding its position within large-scale dimensions of cortical organization. A dominant, anteroposterior, connectivity mode represented a gradual shift in connectivity from default, sensorimotor and temporolimbic regions toward occipital and frontoparietal areas, whereas a secondary mode separated the middle hippocampus from anterior and posterior ends, on the basis of a shift in connectivity from cortical association areas to primary sensory and somatomotor regions. Importantly, we show that a youth-like gradient profile in older age, i.e. maintained distinctiveness of connectivity along gradients, is linked to superior mnemonic function, emphasizing age-related loss of specificity in gradient topography as a hippocampal marker of age-related memory decline. Collectively, our results underscore the important contribution of disentangling multiple dimensions of hippocampal functional organization in advancing our understanding of cortico-hippocampal systems for memory and behavior.

Functional connectivity estimated using resting-state fMRI in humans has successfully provided functional analogues of the hippocampus canonical internal circuitry and its structural connections with cortical areas (Dalton et al., 2019; Ezama et al., 2021; Libby et al., 2012; Maass et al., 2015), at a coarse scale confirming the anteroposterior gradient in

connectivity originally suggested in the animal literature (Aggleton, 2012; Amaral & Witter, 1989; Strange et al., 2014; Witter et al., 1989). Indeed, our observation of a principal anteroposterior gradient converges with a large body of evidence demonstrating, across a variety of methodological approaches, differences in functional cortical connectivity along the hippocampus longitudinal axis (Blessing et al., 2016; Chase et al., 2015; Nordin et al., 2021; Plachti et al., 2019; Poppenk & Moscovitch, 2011; Przeździk et al., 2019; Robinson et al., 2015; Tian et al., 2020; vos de Wael et al., 2018; Zhong et al., 2019). Despite the consistency by which this organizational dimension emerges (Genon et al., 2021), inconsistencies remain in terms of the specific cortical motif it reflects and, in turn, its role in behavior. We propose that inconsistencies in part stem from overlooking multiple overlapping and complementary modes of hippocampal function, not easily distinguishable through traditional parcellation-based approaches, which assume homogeneous function within distinct portions of the hippocampus.

Using connectopic mapping (Haak et al., 2018; Haak & Beckmann, 2020), we link two distinct dimensions of cortical integration to the hippocampus longitudinal axis. The first, we argue, can be interpreted as a local representation of a task-negative/task-positive cortical motif, whereas the second mode as a local map of the principal gradient of unimodal-transmodal cortical organization, previously demonstrated across a wide range of functional, structural and molecular modalities (Hansen et al., 2021; Huntenburg et al., 2018; Margulies et al., 2016; Paquola et al., 2019; Shafiei et al., 2020; Valk et al., 2020). The observation that macroscale relationships between distinct cortical systems are mapped out by the hippocampus may reflect its primordial position in the laminar differentiation characterizing the development of the cerebral cortex (Goulas et al., 2019; Pandya et al., 2015). This supports the notion that the functional organization of the hippocampus stands, from a phylogenetic perspective, to inform general principles of brain organization (Genon et al., 2021; Paquola et al., 2020).

There is currently a lack of consensus regarding the specific topography of hippocampal integration with areas of the default-mode network, also constituting core areas of the brain's system for memory-guided behavior (Ranganath & Ritchey, 2012; Ritchey & Cooper, 2020; Schacter et al., 2007; Spreng et al., 2008). While several studies attribute main default-mode interactions to the posterior hippocampus (Adnan et al., 2016; Ezama et al., 2021; Libby et al., 2012; Poppenk & Moscovitch, 2011; Qin et al., 2016; Ranganath & Ritchey, 2012), consistent with its anatomical connectivity with midline posterior parietal areas, such as the retrosplenial cortex (Aggleton, 2012; Insausti & Muñoz, 2001), other sources emphasize the anterior hippocampus in driving the region's connectivity with default-mode areas (Blessing et al., 2016; Chase et al., 2015; Vogel et al., 2020; Zhong et al., 2019), on the basis of its anatomical connectivity with ventromedial prefrontal areas (Aggleton, 2012). Our results may accommodate both of these accounts.

First, by placing default-mode and frontoparietal areas at opposing ends of a principal anteroposterior gradient, we extend previous gradient-based findings in young adults (Przeździk et al., 2019; Tian et al., 2020; vos de Wael et al., 2018), and contribute to their validation of studies reporting predominant anterior hippocampal connectivity with default-mode areas in parallel to connectivity of the posterior hippocampus to occipital and frontoparietal areas – yielding an anteroposterior differentiation in hippocampal integration with task-negative and task-positive networks (Chase et al., 2015). Second, the second-order gradient highlighted connectivity of the middle hippocampus as separate from that of anterior and posterior regions, distinctively linking it to core regions of the default mode network, namely medial frontal and medial parietal areas. Examining previous findings, this may in fact align with observations of predominant posterior hippocampal connectivity with the default-mode network – as a large number of these studies observe shifts towards medial frontal and parietal connectivity already between anterior and middle hippocampal locations (Ezama et al.,

2021; Kahn et al., 2008; Qin et al., 2016), or use posterior hippocampal parcels encompassing the middle hippocampus after a two-part division at the uncal apex (Adnan et al., 2016; Poppenk & Moscovitch, 2011).

While the principal anteroposterior gradient is well-established in the literature (Genon et al., 2021; Poppenk et al., 2013), demonstrated not only in function (Przeździk et al., 2019; Tian et al., 2020; vos de Wael et al., 2018), but also in structural covariance (Plachti et al., 2019), gene expression (Vogel et al., 2020), and in graded anteroposterior transitions of anatomical connections (Beaujoin et al., 2018; Dalton et al., 2022), the secondary long-axis gradient remains more elusive. Here, we present multiple lines of evidence supporting an interpretation of the second-order gradient as a local representation of the principal gradient of macroscale cortical organization (Huntenburg et al., 2018; Margulies et al., 2016): the unimodal-transmodal distribution of a) large-scale cortical networks in gradient space (Figure 2); b) meta-analytic terms in Neurosynth (Figure 3B); and the spatial correspondence with a functional unimodal-transmodal cortical gradient (Figure 2). Furthermore, topography of this gradient overlapped with topography of hippocampal D1DR distribution, mirroring the organizational overlap between function and D1DR established across the unimodal-transmodal cortical axis (Pedersen et al., 2023). Additionally, we could reliably reproduce this gradient in an independent sample covering the adult lifespan (Supplementary Figure 3), as well as in a sub set of younger participants (Figure 6C).

Applying data-driven multivariate analysis to parcellation-based estimates of hippocampal connectivity, we have previously observed a similar second-order pattern distinguishing connectivity of the middle hippocampus from that shared by anterior and posterior regions, in an age-homogeneous sample of older adults (Nordin et al., 2021). Consistent non-linear transitions along the anteroposterior axis also emerge in other properties of hippocampal function. For instance, inter-voxel similarity – a proxy for processing

granularity (Brunec et al., 2018) – has been reported displaying U-shaped anteroposterior variation, separating middle from anterior and posterior hippocampal areas (Thorp et al., 2022). The overlapping linear and U-shaped long-axis modes observed in the present study might reflect the superimposition of gradients and hubs of anatomical connections indicated in both the human and animal hippocampus (Dalton et al., 2022; Strange et al., 2014).

Consistent with previous gradient-based observations in young adults (Przeździk et al., 2019), we observed an association between topography of the principal gradient and episodic memory in young participants. Behavioral characterizations of the principal, anteroposterior, mode of hippocampal connectivity describe a dimension spanning between self-centric, affective and social vs. world-centric and cognitive poles (Plachti et al., 2019; Vogel et al., 2020). Using meta-analytical decoding in Neurosynth, we observed behavioral transitions largely in line with these observations, and with the interpretation of this gradient as reflecting a task-negative/positive functional axis. While our results are of descriptive character, task-positive terms such as navigation, episodic memory, encoding and recollection, as well as attention and cognitive control mapped on to the posterior end of the gradient, whereas verbal and social terms showed preferential mapping onto the anterior section of the gradient (Figure 3). It is likely that stronger expression of emotional terms would have been observed towards anterior regions of the gradient if subcortical regions such as the amygdala had been included in its computation (Plachti et al., 2019; Vogel et al., 2020).

A main contribution in explaining individual differences in episodic memory across the adult lifespan was however observed for spatial characteristics of the second-order, unimodal-transmodal, gradient. It is noteworthy that meta-analytical decoding of the second-order gradient primarily described the unimodal connectivity patterns of anterior and posterior hippocampal regions, as opposed to the transmodal connectivity pattern of the middle hippocampus, as linked to terms of episodic memory, encoding, and navigation (Figure 3C). Its

role in memory might be considered in light of the hippocampus integration with the ventral visual system, by which it contributes to complex perceptual processes supporting memory (Lee et al., 2012; Turk-Browne, 2019). There is evidence of direct connections of the hippocampus to early visual areas in humans (Huang et al., 2021; Rolls et al., 2022), and recent tractography-based work mapping the density and spatial distribution of streamline endpoints in the hippocampus demonstrates occipital cortex as one of the areas most highly connected to the hippocampus (Dalton et al., 2022). Importantly, streamline endpoints attributed to early visual areas were primarily localized to the posterior hippocampus and to a smaller region in the anterior hippocampus.

Although we restrict our discussion of the third-order gradient due to its relatively low proportion of explained variance, we note that its organization across the hippocampal transverse axis mirrors previous patterns observed in both structure and function (Plachti et al., 2019; Thorp et al., 2022), at a coarse scale separating CA areas from the subiculum. Consistently, cortical patterns belonging to opposite ends of this gradient matched cortical connectivity profiles previously reported for hippocampal subfields (de Flores et al., 2017; Ezama et al., 2021; vos de Wael et al., 2018). While our results reinforce the notion that functional assessments favor detection of the hippocampus anteroposterior organization, in contrast to that determined by its cytoarchitecture (Genon et al., 2021), they suggest that higher-order connectivity modes may indeed carry coarse-scale information about subfield-determined functional organization.

Transitions in connectivity along the hippocampal long-axis, estimated on the basis of subject-level gradient values, revealed that the gradual anteroposterior and middle-to-anterior/posterior connectivity modes conveyed by the principal and second-order gradients were evident across the adult lifespan (Figure 4). Topographic characteristics of these gradients, nevertheless, showed significant age-related variation, such that older age was associated with

less distinct change in connectivity along these long-axis modes (Figure 4). This effect was exacerbated in a sub group of older adults identified as exhibiting an overall aged gradient profile, separated from older adults exhibiting youth-like gradient topography through classification based on gradient parameters (Figure 7A). This observation provides an additional example of increased homogeneity in hippocampal function in older individuals, previously observed in various measures of local functional connectivity (T. M. Harrison et al., 2019; Stark et al., 2021). Current theories view increased functional homogeneity of the hippocampus as a consequence of its functional isolation from cortical areas, arising from tau-driven degeneration of the perforant pathway (T. M. Harrison et al., 2019; Hyman et al., 1984; Salami et al., 2022). Constituting the main source of input to the hippocampus, age-related deterioration of this pathway has previously been demonstrated as leading to impaired mnemonic functioning (Adams et al., 2022; Yassa et al., 2010). Our results indeed emphasize a behaviorally relevant role of maintained gradient distinctiveness, that is, maintained heterogeneity along connectivity modes, demonstrating that older individuals with an aged gradient profile showed less efficient episodic memory compared older individuals with youth-like gradient topography.

Lower distinctiveness of the principal gradient was reflected in an altered gradient organization across cortex, not only in older individuals displaying an exacerbated effect of age, but also in those exhibiting an overall youth-like gradient profile. Indeed, task-negative/task-positive dynamics are known to significantly alter in aging. Less segregation between these brain areas during both task and rest are typically observed in older adults (Grady et al., 2016; Hughes et al., 2020; Pedersen et al., 2021; Spreng et al., 2016), constituting a common example of age-related neural dedifferentiation (Goh, 2011; Koen & Rugg, 2019). Similar dedifferentiation is also evident in numerous psychiatric diseases involving aspects of hippocampal dysfunction (Whitfield-Gabrieli & Ford, 2012; Zhang et al., 2021), like major

depression (Mulders et al., 2015; Wang et al., 2022), schizophrenia (Whitfield-Gabrieli et al., 2009), and Alzheimer's disease (Weiler et al., 2017). There was, however, a main difference in deviation from this dimension observed between older sub groups. The distribution of cortical networks in gradient space indicated a shift towards a unimodal-transmodal organization in youth-like older adults, not evident in the aged older group (Figure 7D). A meaningful role of this shift is indicated by the observation that individual differences in topography of the principal gradient predicted episodic memory in youth-like older adults only. Taken together, while both older sub groups displayed a departure from the task-negative/task-positive cortical motif, emerging as dominant across the sample and in younger adults, only in one of these groups did this reflect a behaviorally relevant shift in cortical integration.

A limitation associated with this study is that our cross-sectional data cannot inform aspects of age-related longitudinal change in hippocampal connectivity modes. While our results demonstrate individual differences in the degree of age-related effects on the distinctiveness of gradients, longitudinal data is required to determine if these differences occur as a result of differential change of over time, and to which extent they involve a true shift in hippocampal cortical integration – as predicted by our observations in older adults displaying a youth-like gradient profile. Whereas longitudinal data is required inform the underlying mechanisms of individual differences in hippocampal gradient topography in older age (Cabeza et al., 2018), our results provide a foundation for further evaluation of them as a potential marker of cognitive decline. It is important to also consider potential limitations arising from the fact that computation of gradients was restricted to hippocampal connectivity with cortical areas. It is likely that the behavioral characterizations of gradients would alter in response to including connectivity with, for instance striatal areas, previously observed to mediate episodic memory (Nordin et al., 2021; Nyberg et al., 2016). Furthermore, whereas connectopic mapping (Haak et al., 2018; Haak & Beckmann, 2020) allows for subject-level parameterization of gradient

topography through spatial statistical modelling, there is currently limited means for statistical inference across the cortical projections of gradients. As such, there is a descriptive quality to some aspects of this study, although thorough measures have been taken to evaluate characteristics of cortical motifs from multiple perspectives. Importantly, gradients showed high correspondence with available previous observations and were reproduced in an independent data set, as well as in a sub group of younger participants.

A lot stands to be gained from applying connectopic mapping to hippocampal cortical integration in additional contexts, characterizing its potential modulation by tasks such as memory encoding/retrieval, spatial navigation, and naturalistic viewing. Particular gain would likely come from gradient mapping in clinical samples. For instance, current studies highlight distinct anteroposterior hippocampal networks as differentially targeted by early tau and β-amyloid (Aβ) pathology (Berron et al., 2020; Maass et al., 2019), and the spread of tau as spatially determined by neural activation and connectivity (Adams et al., 2019; Wu et al., 2016). As most studies still adopt a priori, parcellation-based, definitions of hippocampal regions and networks in combination with univariate approaches to connectivity, gradient mapping may provide valuable multidimensional and topographically more fine-grained insight to these characterizations.

This study demonstrates two overlapping modes of functional connectivity organized along the hippocampus longitudinal axis, each constituting a local representation of a large-scale neocortical motif. Individual differences in the topography of these modes were linked to episodic memory, and suggested shared principles of functional and neuromolecular organization within the hippocampus. Collectively, our results provide a multidimensional framework for understanding hippocampal cortical integration and its contribution to memory across the adult human lifespan.

Methods

This study included data from the DopamiNe, Age, connectoMe, and Cognition (DyNAMiC) study, for which the design and procedures have been described in detail elsewhere (Nordin et al., 2022). Here, we include the materials and methods relevant to the current study. DyNAMiC was approved by the Regional Ethical board and the local Radiation Safety Committee of Umeå, Sweden. All participants provided written informed consent prior to testing.

Participants

The DyNAMiC sample included 180 participants (20-79 years; mean age = 49.8±17.4; 90 men/90 women equally distributed within each decade). Individuals were randomly selected from the population register of Umeå, Sweden, and recruited via postal mail. Exclusion criteria implemented during the recruitment procedure included brain pathology, impaired cognitive functioning (Mini Mental State Examination < 26), medical conditions and treatment that could affect brain functioning and cognition (e.g. dementia, diabetes, and psychiatric diagnosis), and brain imaging contraindications (e.g. metal implants). All participants were native Swedish speakers. A total of 16 participants were excluded from connectopic mapping due to excessive in-scanner motion, leaving resting-state fMRI data for 164 participants (20-78 years; mean age = 48.7±17.3). As a replication data set, we used an independent sample of 224 cognitively healthy and native Swedish-speaking adults (122 men/102 women; 29-85 years mean age = 65.0±13.0) from the population-based Betula project, for which the design and recruitment procedures have been reported in detail elsewhere (Nilsson et al., 2004; Nyberg et al., 2020).

Episodic memory

Episodic memory was measured using three tasks testing word recall, number-word recall and object-location recall, respectively (Nevalainen et al., 2015; Nordin et al., 2022). In the word

recall task, participants were presented with 16 Swedish concrete nouns that appeared successively on a computer screen. Each word was presented for 6 s during encoding with an inter-stimulus interval (ISI) of 1 s. Following encoding, participants reported as many words as they could recall by typing them using the keyboard. Two trials were completed, yielding a maximum score of 32. In the number-word task, participants encoded pairs of 2-digit numbers and concrete plural nouns (e.g., 46 dogs). During encoding, eight number-word pairs were presented, each displayed for 6 s, with an ISI of 1 s. Following encoding, nouns were presented again, in a re-arranged order, and participants had to report the 2-digit number associated with each presented noun (e.g. How many dogs?). This task included two trials with a total maximum score of 16. The third task was an object-location memory task. Here, participants were presented with a 6 × 6 square grid in which 12 objects were, one by one, shown at distinct locations. Each object-position pairing was displayed for 8 s, with an ISI of 1 s. Following encoding, all objects were simultaneously shown next to the grid for the participant to move them (in any order) to their correct position in the grid. If unable to recall the correct position of an object, participants had to guess and place the object in the grid to the best of their ability. Two trials of this task were completed, making the total maximum score 24.

A composite score of performances across the three tasks was calculated and used as the measure of episodic memory. For each of the three tasks, scores were summarized across the total number of trials. The three resulting sum scores were z-standardized and averaged to form one composite score of episodic memory performance (T score: mean = 50; SD = 10). Missing values were replaced by the average of the available observed scores.

Image acquisition

Brain imaging was conducted at Umeå University Hospital, Sweden. Structural and functional MRI data were acquired with a 3T Discovery MR 750 scanner (General Electric, WI, USA),

using a 32-channel head coil. Positron emission tomography (PET) data were acquired with a Discovery PET/CT 690 scanner (General Electric, WI, USA).

Structural MR Imaging

Anatomical T1-weighted images were acquired with a 3D fast-spoiled gradient-echo sequence, collected as 176 slices with a thickness of 1 mm. Repetition time (TR) was 8.2 ms, echo-time (TE) = 3.2 ms, flip angle = 12º, and field of view (FOV) = 250 × 250 mm.

Functional MR Imaging

Functional MR data were collected during resting-state, with participants instructed to keep their eyes open and focus on a fixation cross during scanning. Images were acquired using a T2*-weighted single-shot echo-planar imaging (EPI) sequence, with a total of 350 volumes collected over 12 minutes. The functional time series was sampled with 37 transaxial slices, slice thickness = 3.4 mm, and 0.5 mm spacing, TR = 2000 ms, TE = 30 ms, flip angle = 80º, and FOV = 250 x 250 mm. Ten dummy scans were collected at the start of the sequence.

PET Imaging

PET was conducted in 3D mode with a Discovery PET/CT 690 (General Electric, WI, US) to assess whole-brain D1 receptor availability using the radioligand [^{11}C]SCH23390. Scanning was done during a resting condition, with participants instructed to lay still and remain awake with their eyes open. To minimize head movement, a thermoplastic mask (Posicast®; CIVCO medical solutions; IA, US) was individually fitted for each participant, and attached to the bed surface during scanning. Following a low-dose CT scan (10 mA, 120 kV, and 0.8 s rotation time) for attenuation correction, an intravenous bolus injection with target radioactivity of 350 MBq [^{11}C]SCH23390 was administered. The PET scan was a 60 min dynamic scan, with 6 x

10 s, 6 x 20 s, 6 x 40 s, 9 x 60 s, 22 x 120 s frames. The average radioactivity dose administered to participants was 337±27 MBq (range 205-391 MBq). Due to participant drop-out and technical issues, complete PET data was available for 177 DyNAMiC participants.

Image preprocessing

Hippocampal segmentation and volumetric assessment

Individual anatomical T1-weighted images were submitted to automated segmentation in FreeSurfer version 6 (Fischl et al., 2002, 2004). A mean image of participants' normalized T1-weighted images was also segmented in FreeSurfer, and yielded hippocampal and cortical segmentations used as masks for connectopic mapping. Regional gray matter (GM) volume was estimated from subject-specific hippocampal segmentations, and were corrected for total intracranial volume (ICV; the sum of volumes for grey matter, white matter, and cerebrospinal fluid). Adjusted volumes were equal to the raw volume - b(ICV - mean ICV), where b is the regression slope of volume on ICV (Buckner et al., 2004; Jack et al., 1989). Automated segmentation of the hippocampus into subiculum, CA1-3, and DG/CA4 subfields was conducted in FreeSurfer using the group-average T1-weighted image, for sample-specific masks to overlay onto G3.

Functional MRI data

Resting-state fMRI data were preprocessed using Statistical Parametric Mapping (SPM12: Wellcome Trust Centre for Neuroimaging, http://www.fil.ion.ucl.ac.uk/spm/) implemented in an in-house software, DataZ. Functional images were slice-timing corrected, co-registered to to the anatomical T1-images, and motion corrected, and underwent distortion correction using subject-specific B0-field maps. The functional data were subsequently co-registered to the anatomical T1-images again, temporally demeaned and linear and quadratic effects were

removed. Next, a 36-parameter nuisance regression model was applied (Ciric et al., 2017), including mean cerebrospinal, white-matter, and whole-brain signal in addition to six motion parameters, including parameters' squares, derivatives, and squared derivatives. To further control for in-scanner motion, the model also included a set of spike regressors, defined as binary vectors of motion-contaminated volumes exceeding a volume-to-volume root-mean-squared (RMS) displacement of 0.25 mm (Satterthwaite et al., 2013). A temporal high-pass filter (with a threshold of 0.009 Hz) was applied simultaneously as nuisance regression in order to not re-introduce nuisance signals (Hallquist et al., 2013). Finally, images were normalized to MNI space by Diffeomorphic Anatomical Registration using Exponentiated Lie algebra (DARTEL: Ashburner, 2007) and smoothed with a 6-mm FWHM Gaussian kernel. Four individuals were excluded from the template-generation step due to non-pathological anatomical irregularities. In total, 16 participants were excluded due to displaying excessive in-scanner motion, as defined by displaying i) more than 20 volumes with >0.25 relative RMS difference in motion, and ii) greater than 0.2 average RMS across the run. On average, the relative RMS difference in motion across the sample was 0.090 (± 0.063), and the mean frame-wise displacement (FD) was 0.164 (± 0.104).

Dopamine D1 receptor availability

Preprocessing of PET data was performed in SPM12 (Wellcome Trust Centre for Neuroimaging, http://www.fil.ion.ucl.ac.uk/spm/). Binding potential relative to non-displaceable binding in a reference region (BP_{ND}; Innis et al., 2007), was used as an estimate of receptor availability (i.e. D1DR) in the hippocampus, for each participant defined using the FreeSurfer segmentation of their anatomical images. Cerebellum was used as reference region. PET images were corrected for head movement by using frame-to-frame image co-registration, and co-registered with T1-weighted MRI images with re-slicing to T1 voxel size. The simplified

reference-tissue model (SRTM) was used to model regional time-activity course (TAC) data (Lammertsma & Hume, 1996). Regional TAC data were adjusted for partial volume effects (PVE) by using the symmetric geometric transfer matrix (SGTM) method implemented in FreeSurfer (Greve et al., 2016), and an estimated point-spread-function of 2.5 mm full-width-at-half-maximum (FWHM).

Mapping gradients of functional connectivity

Connectopic mapping (Haak et al., 2018) was run through the ConGrads toolbox (Haak et al., 2018; Haak & Beckmann, 2020) implemented in FSL (Jenkinson et al., 2012; Smith et al., 2004). Mapping was conducted on both subject level and group level, for the left and right hippocampus separately, and involved two main steps. First, for every hippocampal voxel, connectivity fingerprints were computed as the Pearson correlation between the voxel-wise time-series and a singular-value decomposition (SVD) representation of all cortical voxels. In a second step, non-linear manifold learning (Laplacian eigenmaps) was applied to a matrix expressing the degree of similarity between the voxel-wise fingerprints. This yields eigenvectors, so called connectopic maps, representing modes of functional connectivity (i.e. functional gradients). Each connectopic map is then projected onto cortex, for which each vertex is color coded according to the voxel in the hippocampus it correlates the most with. Since connectopic mapping at group level involves applying Laplacian eigenmaps to a group-average similarity matrix, group level mapping across the sample was conducted using the hippocampal and cortical masks derived from the FreeSurfer segmentation of a sample-mean structural image. Mapping was specified to compute 20 gradients, and a subsequent scree plot over explained variance indicated meaningful contributions of the three first connectopic maps, together explaining 67% of the variance across hemispheres (Supplementary Figure 1).

Alignment of connectopic maps across participants

To ensure optimal alignment of identified connectopic maps across participants, we employed Procrustes alignment, based on voxel-wise correlations, to order subject-level connectopic maps according to their correspondence with a set of reference maps (i.e. gradients computed at group level across the full sample). Moreover, whereas the sign of connectopic maps is arbitrary, differences therein have an impact on the spatial model parameters describing the topographic characteristics of gradients, derived through TSM in a later step. As such, the sign of subject-level connectopic maps showing negative correlations with the corresponding group-level reference map were inversed.

Trend surface modelling

Using spatial statistics, the topography of a connectopic map can be represented by a small number of spatial model parameters. This parameterization of gradients enables analyses of inter-individual differences, and is achieved through trend surface modelling (TSM), implemented in a third step of the ConGrads analysis pipeline (Haak et al., 2018). In this step, the spatial pattern of each subject-level connectopic map is approximated by estimating a spatial statistical model. Model estimation involves fitting a set of polynomial basis functions along canonical axes of the connectopic map. In MNI space, this entails estimation along x, y, and z axes of the hippocampus. Thus, fitting a polynomial of degree 1 yields three TSM parameters (x, y, z), with any increase in model order corresponding to an increase in number of parameters (e.g. 6 parameters for the second model order: x, y, z, x^2, y^2, z^2; 9 parameters for the third model order, etc.). Trend surface models are fitted with an increasing polynomial degree using Bayesian linear regression, which provides likelihood estimates that can be used for subsequent model selection. Here, we conducted model selection based on three information sources: a) the Bayesian Information Criterion (BIC) across subjects for models estimated at orders 1-10;

b) the % explained variance in connectopic maps by each model; and c) visual inspection of group-level gradients reconstructed from TSM parameters at different model orders. The purpose of using multiple information sources, as opposed to simply BIC, was to find a trade-off between high-quality reconstructions of gradients by TSM models, while keeping the number of model parameters sufficiently low for multivariate statistical analyses. A model order of 3 (=9 TSM parameters) was selected for G1, whereas a model order of 4 (=12 TSM parameters) was selected for G2 and G3 (Supplementary Figure 5). Each gradient's set of TSM parameters were then used as either dependent or independent variables in multivariate GLMs investigating links between gradient topography and variables such as age, episodic memory performance, and D1DR distribution.

Transitions in connectivity as a function of the hippocampal longitudinal axis

To visualize the orthogonal patterns of change in connectivity conveyed by each gradient, and to aid in the interpretation of age effects, we divided each subject-level connectopic map into 23 bins of ~2mm along the hippocampus anterior-posterior axis and estimated the average gradient value (ranging from 0-1) for each bin. Plotting the values of each bin against their distance in mm from the most anterior voxel in the hippocampus as such demonstrates the pattern of change in connectivity along the anterior-posterior axis (Przeździk et al., 2019).

Correlations between hippocampal gradients and the principal unimodal-transmodal gradient of cortical function

Spearman correlations were computed between each hippocampal gradient and a unimodal-transmodal gradient of cortical function previously reported in the DyNAMiC sample (Pedersen et al., 2023). To ensure sufficient alignment of gradients' cortical projections and the cortical gradient, all surfaces were resampled according to the 400-parcel Schaefer atlas (Schaefer et

al., 2018). Statistical significance of correlations was assessed by spin-test permutation (Alexander-Bloch et al., 2018), randomly rotating a spherical projection of the cortical maps 1000 times, with two-tailed statistical significance determined at a 95% confidence level.

Mapping behavioral transitions along gradients using Neurosynth

Transitions in behavioral domains were mapped onto G1 and G2 using meta-analytical decoding in Neurosynth (Yarkoni et al., 2011). We assessed two sets of behavioral terms (Figure 3), the first was a selection of terms commonly linked to anteroposterior hippocampal functional specialization (Grady, 2019; Plachti et al., 2019), and the second a selection of terms based on a previous report demonstrating behavioral transitions along a unimodal-transmodal cortical axis (Margulies et al., 2016). For correspondence with meta-analytical maps, we created region of interest masks by projecting the cortical surface of each gradient to the 2-mm volumetric MNI152 standard space. These volumetric images were then divided into five twenty-percentile bins and binarized. The resulting images were used as input to the Neurosynth decoder, yielding an *r* statistic associated with each selected behavioral term per section of each gradient.

Acknowledgements

This work was supported by the Swedish Research Council (grant number 2016-01936 to A.S.), Riksbankens Jubileumsfond (grant number P20-0515 to A.S.), Knut and Alice Wallenberg Foundation (Wallenberg Fellow grant to A.S.), and StratNeuro grant at Karolinska Institutet (A.S.). The Betula Study is supported by a Scholar grant to L.N. from the Knut and Alice Wallenberg Foundation. FreeSurfer calculations were enabled by resources provided by the Swedish National Infrastructure for Computing (SNIC) at HPC2N, partially funded by the Swedish Research Council through grant agreement no. 2018-05973.

References

Adams, J. N., Kim, S., Rizvi, B., Sathishkumar, M., Taylor, L., Harris, A. L., Mikhail, A., Keator, D. B., McMillan, L., & Yassa, M. A. (2022). Entorhinal–Hippocampal Circuit Integrity Is Related to Mnemonic Discrimination and Amyloid-β Pathology in Older Adults. *Journal of Neuroscience*, *42*(46), 8742–8753. https://doi.org/10.1523/JNEUROSCI.1165-22.2022

Adams, J. N., Maass, A., Harrison, T. M., Baker, S. L., & Jagust, W. J. (2019). Cortical tau deposition follows patterns of entorhinal functional connectivity in aging. *ELife*, *8*, e49132. https://doi.org/10.7554/eLife.49132

Adnan, A., Barnett, A., Moayedi, M., McCormick, C., Cohn, M., & McAndrews, M. P. (2016). Distinct hippocampal functional networks revealed by tractography-based parcellation. *Brain Structure and Function*, *221*(6), 2999–3012. https://doi.org/10.1007/s00429-015-1084-x

Aggleton, J. P. (2012). Multiple anatomical systems embedded within the primate medial temporal lobe: Implications for hippocampal function. *Neuroscience & Biobehavioral Reviews*, *36*(7), 1579–1596. https://doi.org/10.1016/j.neubiorev.2011.09.005

Alexander-Bloch, A. F., Shou, H., Liu, S., Satterthwaite, T. D., Glahn, D. C., Shinohara, R. T., Vandekar, S. N., & Raznahan, A. (2018). On testing for spatial correspondence between maps of human brain structure and function. *NeuroImage*, *178*, 540–551. https://doi.org/10.1016/j.neuroimage.2018.05.070

Amaral, D. G., & Witter, M. P. (1989). The three-dimensional organization of the hippocampal formation: A review of anatomical data. *Neuroscience*, *31*(3), 571–591. https://doi.org/10.1016/0306-4522(89)90424-7

Amunts, K., Kedo, O., Kindler, M., Pieperhoff, P., Mohlberg, H., Shah, N. J., Habel, U., Schneider, F., & Zilles, K. (2005). Cytoarchitectonic mapping of the human amygdala, hippocampal region and entorhinal cortex: Intersubject variability and probability maps. *Anatomy and Embryology*, *210*(5–6), 343–352. https://doi.org/10.1007/s00429-005-0025-5

Ashburner, J. (2007). A fast diffeomorphic image registration algorithm. *NeuroImage*, *38*(1), 95–113. https://doi.org/10.1016/j.neuroimage.2007.07.007

Barnes, J., Bartlett, J. W., van de Pol, L. A., Loy, C. T., Scahill, R. I., Frost, C., Thompson, P., & Fox, N. C. (2009). A meta-analysis of hippocampal atrophy rates in Alzheimer's disease. *Neurobiology of Aging*, *30*(11), 1711–1723. https://doi.org/10.1016/j.neurobiolaging.2008.01.010

Beaujoin, J., Palomero-Gallagher, N., Boumezbeur, F., Axer, M., Bernard, J., Poupon, F., Schmitz, D., Mangin, J.-F., & Poupon, C. (2018). Post-mortem inference of the human hippocampal connectivity and microstructure using ultra-high field diffusion MRI at 11.7 T. *Brain Structure and Function*, *223*(5), 2157–2179. https://doi.org/10.1007/s00429-018-1617-1

Berron, D., van Westen, D., Ossenkoppele, R., Strandberg, O., & Hansson, O. (2020). Medial temporal lobe connectivity and its associations with cognition in early Alzheimer's disease. *Brain*, *143*(4), 1233–1248. https://doi.org/10.1093/brain/awaa068

Berron, D., Vogel, J. W., Insel, P. S., Pereira, J. B., Xie, L., Wisse, L. E. M., Yushkevich, P. A., Palmqvist, S., Mattsson-Carlgren, N., Stomrud, E., Smith, R., Strandberg, O., & Hansson, O. (2021). Early stages of tau pathology and its associations with functional connectivity, atrophy and memory. *Brain*, *144*(9), 2771–2783. https://doi.org/10.1093/brain/awab114

Blessing, E. M., Beissner, F., Schumann, A., Brünner, F., & Bär, K.-J. (2016). A data-driven approach to mapping cortical and subcortical intrinsic functional connectivity along the longitudinal hippocampal axis. *Human Brain Mapping*, *37*(2), 462–476. https://doi.org/10.1002/hbm.23042

Braak, H., & Braak, E. (1991). Neuropathological stageing of Alzheimer-related changes. *Acta Neuropathologica*, *82*(4), 239–259. https://doi.org/10.1007/BF00308809

Brunec, I. K., Bellana, B., Ozubko, J. D., Man, V., Robin, J., Liu, Z.-X., Grady, C., Rosenbaum, R. S., Winocur, G., Barense, M. D., & Moscovitch, M. (2018). Multiple scales of representation along the hippocampal anteroposterior axis in humans. *Current Biology*, *28*(13), 2129-2135.e6. https://doi.org/10.1016/j.cub.2018.05.016

Buckner, R. L., Head, D., Parker, J., Fotenos, A. F., Marcus, D., Morris, J. C., & Snyder, A. Z. (2004). A unified approach for morphometric and functional data analysis in young, old, and

demented adults using automated atlas-based head size normalization: Reliability and validation against manual measurement of total intracranial volume. *NeuroImage*, *23*(2), 724–738. https://doi.org/10.1016/j.neuroimage.2004.06.018

Burgess, N., Maguire, E. A., & O'Keefe, J. (2002). The human hippocampus and spatial and episodic memory. *Neuron*, *35*(4), 625–641. https://doi.org/10.1016/S0896-6273(02)00830-9

Cabeza, R., Albert, M., Belleville, S., Craik, F. I. M., Duarte, A., Grady, C. L., Lindenberger, U., Nyberg, L., Park, D. C., Reuter-Lorenz, P. A., Rugg, M. D., Steffener, J., & Rajah, M. N. (2018). Maintenance, reserve and compensation: The cognitive neuroscience of healthy ageing. *Nature Reviews Neuroscience*, *19*(11), 701. https://doi.org/10.1038/s41583-018-0068-2

Campbell, S., & MacQueen, G. (2004). The role of the hippocampus in the pathophysiology of major depression. *Journal of Psychiatry and Neuroscience*, *29*(6), 417–426.

Chase, H. W., Clos, M., Dibble, S., Fox, P., Grace, A. A., Phillips, M. L., & Eickhoff, S. B. (2015). Evidence for an anterior–posterior differentiation in the human hippocampal formation revealed by meta-analytic parcellation of fMRI coordinate maps: Focus on the subiculum. *NeuroImage*, *113*, 44–60. https://doi.org/10.1016/j.neuroimage.2015.02.069

Ciric, R., Wolf, D. H., Power, J. D., Roalf, D. R., Baum, G. L., Ruparel, K., Shinohara, R. T., Elliott, M. A., Eickhoff, S. B., Davatzikos, C., Gur, R. C., Gur, R. E., Bassett, D. S., & Satterthwaite, T. D. (2017). Benchmarking of participant-level confound regression strategies for the control of motion artifact in studies of functional connectivity. *NeuroImage*, *154*, 174–187. https://doi.org/10.1016/j.neuroimage.2017.03.020

Dalton, M. A., D'Souza, A., Lv, J., & Calamante, F. (2022). New insights into anatomical connectivity along the anterior–posterior axis of the human hippocampus using in vivo quantitative fibre tracking. *ELife*, *11*, e76143. https://doi.org/10.7554/eLife.76143

Dalton, M. A., McCormick, C., & Maguire, E. A. (2019). Differences in functional connectivity along the anterior-posterior axis of human hippocampal subfields. *NeuroImage*, *192*, 38–51. https://doi.org/10.1016/j.neuroimage.2019.02.066

de Flores, R., Das, S. R., Xie, L., Wisse, L. E. M., Lyu, X., Shah, P., Yushkevich, P. A., & Wolk, D. A. (2022). Medial Temporal Lobe Networks in Alzheimer's Disease: Structural and Molecular Vulnerabilities. *Journal of Neuroscience*, *42*(10), 2131–2141. https://doi.org/10.1523/JNEUROSCI.0949-21.2021

de Flores, R., Mutlu, J., Bejanin, A., Gonneaud, J., Landeau, B., Tomadesso, C., Mézenge, F., de La Sayette, V., Eustache, F., & Chételat, G. (2017). Intrinsic connectivity of hippocampal subfields in normal elderly and mild cognitive impairment patients. *Human Brain Mapping*, *38*(10), 4922–4932. https://doi.org/10.1002/hbm.23704

Dubovyk, V., & Manahan-Vaughan, D. (2019). Gradient of expression of dopamine D2 receptors along the dorso-ventral axis of the hippocampus. *Frontiers in Synaptic Neuroscience*, *11*. https://doi.org/10.3389/fnsyn.2019.00028

Edelmann, E., & Lessmann, V. (2018). Dopaminergic innervation and modulation of hippocampal networks. *Cell and Tissue Research*, *373*(3), 711–727. https://doi.org/10.1007/s00441-018-2800-7

Eichenbaum, H. (2000). A cortical–hippocampal system for declarative memory. *Nature Reviews Neuroscience*, *1*(1), 41–50. https://doi.org/10.1038/35036213

El-Ghundi, M., O'Dowd, B. F., & George, S. R. (2007). Insights into the role of dopamine receptor systems in learning and memory. *Reviews in the Neurosciences*, *18*(1), 37–66. https://doi.org/10.1515/revneuro.2007.18.1.37

Ezama, L., Hernández-Cabrera, J. A., Seoane, S., Pereda, E., & Janssen, N. (2021). Functional connectivity of the hippocampus and its subfields in resting-state networks. *The European Journal of Neuroscience*, *53*(10), 3378–3393. https://doi.org/10.1111/ejn.15213

Fischl, B., Salat, D. H., Busa, E., Albert, M., Dieterich, M., Haselgrove, C., van der Kouwe, A., Killiany, R., Kennedy, D., Klaveness, S., Montillo, A., Makris, N., Rosen, B., & Dale, A. M. (2002). Whole brain segmentation: Automated labeling of neuroanatomical structures in the human brain. *Neuron*, *33*(3), 341–355. https://doi.org/10.1016/S0896-6273(02)00569-X

Fischl, B., Salat, D. H., van der Kouwe, A. J. W., Makris, N., Ségonne, F., Quinn, B. T., & Dale, A. M. (2004). Sequence-independent segmentation of magnetic resonance images. *NeuroImage*, *23, Supplement 1*, S69–S84. https://doi.org/10.1016/j.neuroimage.2004.07.016

Gasbarri, A., Verney, C., Innocenzi, R., Campana, E., & Pacitti, C. (1994). Mesolimbic dopaminergic neurons innervating the hippocampal formation in the rat: A combined retrograde tracing and immunohistochemical study. *Brain Research*, *668*(1), 71–79. https://doi.org/10.1016/0006-8993(94)90512-6

Ge, R., Kot, P., Liu, X., Lang, D. J., Wang, J. Z., Honer, W. G., & Vila-Rodriguez, F. (2019). Parcellation of the human hippocampus based on gray matter volume covariance: Replicable results on healthy young adults. *Human Brain Mapping*, *0*(0). https://doi.org/10.1002/hbm.24628

Genon, S., Bernhardt, B. C., La Joie, R., Amunts, K., & Eickhoff, S. B. (2021). The many dimensions of human hippocampal organization and (dys)function. *Trends in Neurosciences*. https://doi.org/10.1016/j.tins.2021.10.003

Goh, J. O. S. (2011). Functional Dedifferentiation and Altered Connectivity in Older Adults: Neural Accounts of Cognitive Aging. *Aging and Disease*, *2*(1), 30–48.

Goulas, A., Margulies, D. S., Bezgin, G., & Hilgetag, C. C. (2019). The architecture of mammalian cortical connectomes in light of the theory of the dual origin of the cerebral cortex. *Cortex*, *118*, 244–261. https://doi.org/10.1016/j.cortex.2019.03.002

Grady, C. (2019). Meta-analytic and functional connectivity evidence from functional magnetic resonance imaging for an anterior to posterior gradient of function along the hippocampal axis. *Hippocampus*, *2019*, 1–16. https://doi.org/10.1002/hipo.23164

Grady, C., Sarraf, S., Saverino, C., & Campbell, K. (2016). Age differences in the functional interactions among the default, frontoparietal control, and dorsal attention networks. *Neurobiology of Aging*, *41*, 159–172. https://doi.org/10.1016/j.neurobiolaging.2016.02.020

Greve, D. N., Salat, D. H., Bowen, S. L., Izquierdo-Garcia, D., Schultz, A. P., Catana, C., Becker, J. A., Svarer, C., Knudsen, G. M., Sperling, R. A., & Johnson, K. A. (2016). Different partial volume correction methods lead to different conclusions: An 18F-FDG-PET study of aging. *NeuroImage*, *132*, 334–343. https://doi.org/10.1016/j.neuroimage.2016.02.042

Haak, K. V., & Beckmann, C. F. (2020). Understanding brain organisation in the face of functional heterogeneity and functional multiplicity. *NeuroImage*, *220*, 117061. https://doi.org/10.1016/j.neuroimage.2020.117061

Haak, K. V., Marquand, A. F., & Beckmann, C. F. (2018). Connectopic mapping with resting-state fMRI. *NeuroImage*, *170*, 83–94. https://doi.org/10.1016/j.neuroimage.2017.06.075

Hallquist, M. N., Hwang, K., & Luna, B. (2013). The nuisance of nuisance regression: Spectral misspecification in a common approach to resting-state fMRI preprocessing reintroduces noise and obscures functional connectivity. *NeuroImage*, *82*, 208–225. https://doi.org/10.1016/j.neuroimage.2013.05.116

Hansen, J. Y., Markello, R. D., Vogel, J. W., Seidlitz, J., Bzdok, D., & Misic, B. (2021). Mapping gene transcription and neurocognition across human neocortex. *Nature Human Behaviour*, *5*(9), Article 9. https://doi.org/10.1038/s41562-021-01082-z

Harrison, P. J. (2004). The hippocampus in schizophrenia: A review of the neuropathological evidence and its pathophysiological implications. *Psychopharmacology*, *174*(1), 151–162. https://doi.org/10.1007/s00213-003-1761-y

Harrison, T. M., Maass, A., Adams, J. N., Du, R., Baker, S. L., & Jagust, W. J. (2019). Tau deposition is associated with functional isolation of the hippocampus in aging. *Nature Communications*, *10*(1), Article 1. https://doi.org/10.1038/s41467-019-12921-z

Huang, C.-C., Rolls, E. T., Hsu, C.-C. H., Feng, J., & Lin, C.-P. (2021). Extensive Cortical Connectivity of the Human Hippocampal Memory System: Beyond the "What" and "Where" Dual Stream Model. *Cerebral Cortex*, *31*(10), 4652–4669. https://doi.org/10.1093/cercor/bhab113

Hughes, C., Faskowitz, J., Cassidy, B. S., Sporns, O., & Krendl, A. C. (2020). Aging relates to a disproportionately weaker functional architecture of brain networks during rest and task states. *NeuroImage*, *209*, 116521. https://doi.org/10.1016/j.neuroimage.2020.116521

Huntenburg, J. M., Bazin, P.-L., & Margulies, D. S. (2018). Large-Scale Gradients in Human Cortical Organization. *Trends in Cognitive Sciences*, *22*(1), 21–31. https://doi.org/10.1016/j.tics.2017.11.002

Hyman, B. T., Van Hoesen, G. W., Damasio, A. R., & Barnes, C. L. (1984). Alzheimer's Disease: Cell-Specific Pathology Isolates the Hippocampal Formation. *Science*, *225*(4667), 1168–1170. https://doi.org/10.1126/science.6474172

Innis, R. B., Cunningham, V. J., Delforge, J., Fujita, M., Gjedde, A., Gunn, R. N., Holden, J., Houle, S., Huang, S.-C., Ichise, M., Iida, H., Ito, H., Kimura, Y., Koeppe, R. A., Knudsen, G. M., Knuuti, J., Lammertsma, A. A., Laruelle, M., Logan, J., … Carson, R. E. (2007). Consensus Nomenclature for in vivo Imaging of Reversibly Binding Radioligands: *Journal of Cerebral Blood Flow & Metabolism*, *27*(27), 1533–1539. https://doi.org/10.1038/sj.jcbfm.9600493

Insausti, R., & Muñoz, M. (2001). Cortical projections of the non-entorhinal hippocampal formation in the cynomolgus monkey (Macaca fascicularis). *European Journal of Neuroscience*, *14*(3), 435–451. https://doi.org/10.1046/j.0953-816x.2001.01662.x

Ishikawa, K., Ott, T., & McGaugh, J. L. (1982). Evidence for dopamine as a transmitter in dorsal hippocampus. *Brain Research*, *232*(1), 222–226. https://doi.org/10.1016/0006-8993(82)90630-8

Jack, C. R., Twomey, C. K., Zinsmeister, A. R., Sharbrough, F. W., Petersen, R. C., & Cascino, G. D. (1989). Anterior temporal lobes and hippocampal formations: Normative volumetric measurements from MR images in young adults. *Radiology*, *172*(2), 549–554. https://doi.org/10.1148/radiology.172.2.2748838

Jenkinson, M., Beckmann, C. F., Behrens, T. E. J., Woolrich, M. W., & Smith, S. M. (2012). FSL. *NeuroImage*, *62*(2), 782–790. https://doi.org/10.1016/j.neuroimage.2011.09.015

Kahn, I., Andrews-Hanna, J. R., Vincent, J. L., Snyder, A. Z., & Buckner, R. L. (2008). Distinct cortical anatomy linked to subregions of the medial temporal lobe revealed by intrinsic functional connectivity. *Journal of Neurophysiology*, *100*(1), 129–139. https://doi.org/10.1152/jn.00077.2008

Kahn, I., & Shohamy, D. (2013). Intrinsic connectivity between the hippocampus, nucleus accumbens and ventral tegmental area in humans. *Hippocampus*, *23*(3), 187–192. https://doi.org/10.1002/hipo.22077

Kempadoo, K. A., Mosharov, E. V., Choi, S. J., Sulzer, D., & Kandel, E. R. (2016). Dopamine release from the locus coeruleus to the dorsal hippocampus promotes spatial learning and memory. *Proceedings of the National Academy of Sciences*, *113*(51), 14835–14840. https://doi.org/10.1073/pnas.1616515114

Koen, J. D., & Rugg, M. D. (2019). Neural Dedifferentiation in the Aging Brain. *Trends in Cognitive Sciences*, *23*(7), 547–559. https://doi.org/10.1016/j.tics.2019.04.012

Lammertsma, A. A., & Hume, S. P. (1996). Simplified Reference Tissue Model for PET Receptor Studies. *NeuroImage*, *4*(3), 153–158. https://doi.org/10.1006/nimg.1996.0066

Laurita, A. C., & Spreng, N. (2017). The Hippocampus and Social Cognition. In D. E. Hannula & M. C. Duff (Eds.), *The Hippocampus from Cells to Systems: Structure, Connectivity, and Functional Contributions to Memory and Flexible Cognition* (pp. 537–558). Springer International Publishing. https://doi.org/10.1007/978-3-319-50406-3_17

Lee, A., Yeung, L.-K., & Barense, M. (2012). The hippocampus and visual perception. *Frontiers in Human Neuroscience*, *6*. https://www.frontiersin.org/articles/10.3389/fnhum.2012.00091

Libby, L. A., Ekstrom, A. D., Ragland, J. D., & Ranganath, C. (2012). Differential connectivity of perirhinal and parahippocampal cortices within human hippocampal subregions revealed by high-resolution functional imaging. *Journal of Neuroscience*, *32*(19), 6550–6560. https://doi.org/10.1523/JNEUROSCI.3711-11.2012

Lieberman, J. A., Girgis, R. R., Brucato, G., Moore, H., Provenzano, F., Kegeles, L., Javitt, D., Kantrowitz, J., Wall, M. M., Corcoran, C. M., Schobel, S. A., & Small, S. A. (2018). Hippocampal dysfunction in the pathophysiology of schizophrenia: A selective review and hypothesis for early detection and intervention. *Molecular Psychiatry*, *23*(8), Article 8. https://doi.org/10.1038/mp.2017.249

Lladó, A., Tort-Merino, A., Sánchez-Valle, R., Falgàs, N., Balasa, M., Bosch, B., Castellví, M., Olives, J., Antonell, A., & Hornberger, M. (2018). The hippocampal longitudinal axis—

Relevance for underlying tau and TDP-43 pathology. *Neurobiology of Aging*, *70*, 1–9. https://doi.org/10.1016/j.neurobiolaging.2018.05.035

Maass, A., Berron, D., Harrison, T. M., Adams, J. N., La Joie, R., Baker, S., Mellinger, T., Bell, R. K., Swinnerton, K., Inglis, B., Rabinovici, G. D., Düzel, E., & Jagust, W. J. (2019). Alzheimer's pathology targets distinct memory networks in the ageing brain. *Brain*, *142*(8), 2492–2509. https://doi.org/10.1093/brain/awz154

Maass, A., Berron, D., Libby, L. A., Ranganath, C., & Düzel, E. (2015). Functional subregions of the human entorhinal cortex. *ELife*, *4*, e06426. https://doi.org/10.7554/eLife.06426

Margulies, D. S., Ghosh, S. S., Goulas, A., Falkiewicz, M., Huntenburg, J. M., Langs, G., Bezgin, G., Eickhoff, S. B., Castellanos, F. X., Petrides, M., Jefferies, E., & Smallwood, J. (2016). Situating the default-mode network along a principal gradient of macroscale cortical organization. *Proceedings of the National Academy of Sciences*, *113*(44), 12574–12579. https://doi.org/10.1073/pnas.1608282113

Moscovitch, M., Cabeza, R., Winocur, G., & Nadel, L. (2016). Episodic memory and beyond: The hippocampus and neocortex in transformation. *Annual Review of Psychology*, *67*(1), 105–134. https://doi.org/10.1146/annurev-psych-113011-143733

Mulders, P. C., van Eijndhoven, P. F., Schene, A. H., Beckmann, C. F., & Tendolkar, I. (2015). Resting-state functional connectivity in major depressive disorder: A review. *Neuroscience & Biobehavioral Reviews*, *56*, 330–344. https://doi.org/10.1016/j.neubiorev.2015.07.014

Nadel, L., & Peterson, M. A. (2013). The hippocampus: Part of an interactive posterior representational system spanning perceptual and memorial systems. *Journal of Experimental Psychology: General*, *142*(4), 1242–1254. https://doi.org/10.1037/a0033690

Nevalainen, N., Riklund, K., Andersson, M., Axelsson, J., Ögren, M., Lövdén, M., Lindenberger, U., Bäckman, L., & Nyberg, L. (2015). COBRA: A prospective multimodal imaging study of dopamine, brain structure and function, and cognition. *Brain Research*, *1612*, 83–103. https://doi.org/10.1016/j.brainres.2014.09.010

Nilsson, L.-G., Adolfsson, R., Bäckman, L., Frias, C. M. de, Molander, B., & Nyberg, L. (2004). Betula: A Prospective Cohort Study on Memory, Health and Aging. *Aging, Neuropsychology, and Cognition*, *11*(2–3), 134–148. https://doi.org/10.1080/13825580490511026

Nordin, K., Gorbach, T., Pedersen, R., Panes Lundmark, V., Johansson, J., Andersson, M., McNulty, C., Riklund, K., Wåhlin, A., Papenberg, G., Kalpouzos, G., Bäckman, L., & Salami, A. (2022). DyNAMiC: A prospective longitudinal study of dopamine and brain connectomes: A new window into cognitive aging. *Journal of Neuroscience Research*, *00*, 1–25. https://doi.org/10.1002/jnr.25039

Nordin, K., Nyberg, L., Andersson, M., Karalija, N., Riklund, K., Bäckman, L., & Salami, A. (2021). Distinct and Common Large-Scale Networks of the Hippocampal Long Axis in Older Age: Links to Episodic Memory and Dopamine D2 Receptor Availability. *Cerebral Cortex*, *31*(7), 3435–3450. https://doi.org/10.1093/cercor/bhab023

Nyberg, L., Andersson, M., Lundquist, A., Salami, A., & Wåhlin, A. (2019). Frontal contribution to hippocampal hyperactivity during memory encoding in aging. *Frontiers in Molecular Neuroscience*, *12*, 1–11. https://doi.org/10.3389/fnmol.2019.00229

Nyberg, L., Boraxbekk, C.-J., Sörman, D. E., Hansson, P., Herlitz, A., Kauppi, K., Ljungberg, J. K., Lövheim, H., Lundquist, A., Adolfsson, A. N., Oudin, A., Pudas, S., Rönnlund, M., Stiernstedt, M., Sundström, A., & Adolfsson, R. (2020). Biological and environmental predictors of heterogeneity in neurocognitive ageing: Evidence from Betula and other longitudinal studies. *Ageing Research Reviews*, *64*, 101184. https://doi.org/10.1016/j.arr.2020.101184

Nyberg, L., Karalija, N., Salami, A., Andersson, M., Wåhlin, A., Kaboovand, N., Köhncke, Y., Axelsson, J., Rieckmann, A., Papenberg, G., Garrett, D. D., Riklund, K., Lövdén, M., Lindenberger, U., & Bäckman, L. (2016). Dopamine D2 receptor availability is linked to hippocampal–caudate functional connectivity and episodic memory. *Proceedings of the National Academy of Sciences*, *113*(28), 7918–7923. https://doi.org/10.1073/pnas.1606309113

Pandya, D., Petrides, M., & Cipolloni, P. B. (2015). *Cerebral Cortex: Architecture, Connections, and the Dual Origin Concept*. Oxford University Press.

Paquola, C., Benkarim, O., DeKraker, J., Larivière, S., Frässle, S., Royer, J., Tavakol, S., Valk, S., Bernasconi, A., Bernasconi, N., Khan, A., Evans, A. C., Razi, A., Smallwood, J., & Bernhardt, B. C. (2020). Convergence of cortical types and functional motifs in the human mesiotemporal lobe. *ELife*, *9*, e60673. https://doi.org/10.7554/eLife.60673

Paquola, C., Wael, R. V. D., Wagstyl, K., Bethlehem, R. A. I., Hong, S.-J., Seidlitz, J., Bullmore, E. T., Evans, A. C., Misic, B., Margulies, D. S., Smallwood, J., & Bernhardt, B. C. (2019). Microstructural and functional gradients are increasingly dissociated in transmodal cortices. *PLOS Biology*, *17*(5), e3000284. https://doi.org/10.1371/journal.pbio.3000284

Pedersen, R., Geerligs, L., Andersson, M., Gorbach, T., Avelar-Pereira, B., Wåhlin, A., Rieckmann, A., Nyberg, L., & Salami, A. (2021). When functional blurring becomes deleterious: Reduced system segregation is associated with less white matter integrity and cognitive decline in aging. *NeuroImage*, *242*, 118449. https://doi.org/10.1016/j.neuroimage.2021.118449

Pedersen, R., Johansson, J., Nordin, K., Rieckmann, A., Wåhlin, A., Nyberg, L., Bäckman, L., & Salami, A. (2023). *Dopamine D1-receptor Organization Contributes to Functional Brain Architecture*. Preprint at bioRxiv.

Persson, J., Stening, E., Nordin, K., & Söderlund, H. (2018). Predicting episodic and spatial memory performance from hippocampal resting-state functional connectivity: Evidence for an anterior–posterior division of function. *Hippocampus*, *28*(1), 53–66. https://doi.org/10.1002/hipo.22807

Plachti, A., Eickhoff, S. B., Hoffstaedter, F., Patil, K. R., Laird, A. R., Fox, P. T., Amunts, K., & Genon, S. (2019). Multimodal parcellations and extensive behavioral profiling tackling the hippocampus gradient. *Cerebral Cortex*, *29*, 1–18. https://doi.org/10.1093/cercor/bhy336

Poppenk, J., Evensmoen, H. R., Moscovitch, M., & Nadel, L. (2013). Long-axis specialization of the human hippocampus. *Trends in Cognitive Sciences*, *17*(5), 230–240. https://doi.org/10.1016/j.tics.2013.03.005

Poppenk, J., & Moscovitch, M. (2011). A hippocampal marker of recollection memory ability among healthy young adults: Contributions of posterior and anterior segments. *Neuron*, *72*(6), 931–937. https://doi.org/10.1016/j.neuron.2011.10.014

Przeździk, I., Faber, M., Fernández, G., Beckmann, C. F., & Haak, K. V. (2019). The functional organisation of the hippocampus along its long axis is gradual and predicts recollection. *Cortex*, *119*, 324–335. https://doi.org/10.1016/j.cortex.2019.04.015

Qin, S., Duan, X., Supekar, K., Chen, H., Chen, T., & Menon, V. (2016). Large-scale intrinsic functional network organization along the long axis of the human medial temporal lobe. *Brain Structure and Function*, *221*(6), 3237–3258. https://doi.org/10.1007/s00429-015-1098-4

Ranganath, C., & Ritchey, M. (2012). Two cortical systems for memory-guided behaviour. *Nature Reviews Neuroscience*, *13*(10), 713–726. https://doi.org/10.1038/nrn3338

Ritchey, M., & Cooper, R. A. (2020). Deconstructing the posterior medial episodic network. *Trends in Cognitive Sciences*, *24*, 451–465. https://doi.org/10.1016/j.tics.2020.03.006

Robinson, J. L., Barron, D. S., Kirby, L. A. J., Bottenhorn, K. L., Hill, A. C., Murphy, J. E., Katz, J. S., Salibi, N., Eickhoff, S. B., & Fox, P. T. (2015). Neurofunctional topography of the human hippocampus. *Human Brain Mapping*, *36*(12), 5018–5037. https://doi.org/10.1002/hbm.22987

Rolls, E. T., Deco, G., Huang, C.-C., & Feng, J. (2022). The effective connectivity of the human hippocampal memory system. *Cerebral Cortex*, *32*(17), 3706–3725. https://doi.org/10.1093/cercor/bhab442

Salami, A., Adolfsson, R., Andersson, M., Blennow, K., Lundquist, A., Adolfsson, A. N., Schöll, M., Zetterberg, H., & Nyberg, L. (2022). Association of APOE ε4 and Plasma p-tau181 with Preclinical Alzheimer's Disease and Longitudinal Change in Hippocampus Function. *Journal of Alzheimer's Disease*, *85*(3), 1309–1320. https://doi.org/10.3233/JAD-210673

Salami, A., Pudas, S., & Nyberg, L. (2014). Elevated hippocampal resting-state connectivity underlies deficient neurocognitive function in aging. *Proceedings of the National Academy of Sciences*, *111*(49), 17654–17659. https://doi.org/10.1073/pnas.1410233111

Salami, A., Wåhlin, A., Kaboodvand, N., Lundquist, A., & Nyberg, L. (2016). Longitudinal evidence for dissociation of anterior and posterior MTL resting-state connectivity in aging: Links to perfusion and memory. *Cerebral Cortex*, *26*(10), 3953–3963. https://doi.org/10.1093/cercor/bhw233

Satterthwaite, T. D., Elliott, M. A., Gerraty, R. T., Ruparel, K., Loughead, J., Calkins, M. E., Eickhoff, S. B., Hakonarson, H., Gur, R. C., Gur, R. E., & Wolf, D. H. (2013). An improved framework for confound regression and filtering for control of motion artifact in the preprocessing of resting-state functional connectivity data. *NeuroImage*, *64*, 240–256. https://doi.org/10.1016/j.neuroimage.2012.08.052

Schacter, D. L., Addis, D. R., & Buckner, R. L. (2007). Remembering the past to imagine the future: The prospective brain. *Nature Reviews Neuroscience*, *8*(9), Article 9. https://doi.org/10.1038/nrn2213

Schaefer, A., Kong, R., Gordon, E. M., Laumann, T. O., Zuo, X.-N., Holmes, A. J., Eickhoff, S. B., & Yeo, B. T. T. (2018). Local-Global Parcellation of the Human Cerebral Cortex from Intrinsic Functional Connectivity MRI. *Cerebral Cortex*, *28*(9), 3095–3114. https://doi.org/10.1093/cercor/bhx179

Shafiei, G., Markello, R. D., Vos de Wael, R., Bernhardt, B. C., Fulcher, B. D., & Misic, B. (2020). Topographic gradients of intrinsic dynamics across neocortex. *ELife*, *9*, e62116. https://doi.org/10.7554/eLife.62116

Small, S. A., Schobel, S. A., Buxton, R. B., Witter, M. P., & Barnes, C. A. (2011). A pathophysiological framework of hippocampal dysfunction in ageing and disease. *Nature Reviews Neuroscience*, *12*(10), 585–601. https://doi.org/10.1038/nrn3085

Smith, S. M., Jenkinson, M., Woolrich, M. W., Beckmann, C. F., Behrens, T. E. J., Johansen-Berg, H., Bannister, P. R., De Luca, M., Drobnjak, I., Flitney, D. E., Niazy, R. K., Saunders, J., Vickers, J., Zhang, Y., De Stefano, N., Brady, J. M., & Matthews, P. M. (2004). Advances in functional and structural MR image analysis and implementation as FSL. *NeuroImage*, *23*, S208–S219. https://doi.org/10.1016/j.neuroimage.2004.07.051

Spreng, R. N., Mar, R. A., & Kim, A. S. N. (2008). The Common Neural Basis of Autobiographical Memory, Prospection, Navigation, Theory of Mind, and the Default Mode: A Quantitative Meta-analysis. *Journal of Cognitive Neuroscience*, *21*(3), 489–510. https://doi.org/10.1162/jocn.2008.21029

Spreng, R. N., Stevens, W. D., Viviano, J. D., & Schacter, D. L. (2016). Attenuated anticorrelation between the default and dorsal attention networks with aging: Evidence from task and rest. *Neurobiology of Aging*, *45*, 149–160. https://doi.org/10.1016/j.neurobiolaging.2016.05.020

Squire, L. R. (2004). Memory systems of the brain: A brief history and current perspective. *Neurobiology of Learning and Memory*, *82*(3), 171–177. https://doi.org/10.1016/j.nlm.2004.06.005

Stark, S. M., Frithsen, A., & Stark, C. E. L. (2021). Age-related alterations in functional connectivity along the longitudinal axis of the hippocampus and its subfields. *Hippocampus*, *31*(1), 11–27. https://doi.org/10.1002/hipo.23259

Strange, B. A., Witter, M. P., Lein, E. S., & Moser, E. I. (2014). Functional organization of the hippocampal longitudinal axis. *Nature Reviews Neuroscience*, *15*(10), 655–669. https://doi.org/10.1038/nrn3785

Thorp, J. N., Gasser, C., Blessing, E., & Davachi, L. (2022). Data-Driven Clustering of Functional Signals Reveals Gradients in Processing Both within the Anterior Hippocampus and across Its Long Axis. *Journal of Neuroscience*, *42*(39), 7431–7441. https://doi.org/10.1523/JNEUROSCI.0269-22.2022

Tian, Y., Margulies, D. S., Breakspear, M., & Zalesky, A. (2020). Topographic organization of the human subcortex unveiled with functional connectivity gradients. *Nature Neuroscience*, *23*(11), Article 11. https://doi.org/10.1038/s41593-020-00711-6

Turk-Browne, N. B. (2019). The hippocampus as a visual area organized by space and time: A spatiotemporal similarity hypothesis. *Vision Research*, *165*, 123–130. https://doi.org/10.1016/j.visres.2019.10.007

Valk, S. L., Xu, T., Margulies, D. S., Masouleh, S. K., Paquola, C., Goulas, A., Kochunov, P., Smallwood, J., Yeo, B. T. T., Bernhardt, B. C., & Eickhoff, S. B. (2020). Shaping brain structure: Genetic and phylogenetic axes of macroscale organization of cortical thickness. *Science Advances*, *6*(39), eabb3417. https://doi.org/10.1126/sciadv.abb3417

Van Essen, D. C., Smith, S. M., Barch, D. M., Behrens, T. E. J., Yacoub, E., & Ugurbil, K. (2013). The WU-Minn Human Connectome Project: An overview. *NeuroImage*, *80*, 62–79. https://doi.org/10.1016/j.neuroimage.2013.05.041

Vermunt, J. K., & Magdison, J. (2002). Latent class cluster analysis. In *Applied latent class analysis* (Vol. 2002, pp. 89–106). Cambridge University Press.

Verney, C., Baulac, M., Berger, B., Alvarez, C., Vigny, A., & Helle, K. B. (1985). Morphological evidence for a dopaminergic terminal field in the hippocampal formation of young and adult rat. *Neuroscience*, *14*(4), 1039–1052. https://doi.org/10.1016/0306-4522(85)90275-1

Vogel, J. W., La Joie, R., Grothe, M. J., Diaz-Papkovich, A., Doyle, A., Vachon-Presseau, E., Lepage, C., Vos de Wael, R., Thomas, R. A., Iturria-Medina, Y., Bernhardt, B., Rabinovici, G. D., & Evans, A. C. (2020). A molecular gradient along the longitudinal axis of the human hippocampus informs large-scale behavioral systems. *Nature Communications*, *11*(1), Article 1. https://doi.org/10.1038/s41467-020-14518-3

vos de Wael, R., Larivière, S., Caldairou, B., Hong, S.-J., Margulies, D. S., Jefferies, E., Bernasconi, A., Smallwood, J., Bernasconi, N., & Bernhardt, B. C. (2018). Anatomical and microstructural determinants of hippocampal subfield functional connectome embedding. *Proceedings of the National Academy of Sciences*, *115*(40), 10154–10159. https://doi.org/10.1073/pnas.1803667115

Wang, Y., Chen, X., Liu, R., Zhang, Z., Zhou, J., Feng, Y., Zeidman, P., Wang, G., & Zhou, Y. (2022). Disrupted effective connectivity of the default, salience and dorsal attention networks in major depressive disorder: A study using spectral dynamic causal modelling of resting-state fMRI. *Journal of Psychiatry and Neuroscience*, *47*(6), E421–E434. https://doi.org/10.1503/jpn.220038

Weiler, M., Campos, B. M. de, Teixeira, C. V. de L., Casseb, R. F., Carletti-Cassani, A. F. M. K., Vicentini, J. E., Magalhães, T. N. C., Talib, L. L., Forlenza, O. V., & Balthazar, M. L. F. (2017). Intranetwork and internetwork connectivity in patients with Alzheimer disease and the association with cerebrospinal fluid biomarker levels. *Journal of Psychiatry and Neuroscience*, *42*(6), 366–377. https://doi.org/10.1503/jpn.160190

Whitfield-Gabrieli, S., & Ford, J. M. (2012). Default Mode Network Activity and Connectivity in Psychopathology. *Annual Review of Clinical Psychology*, *8*(1), 49–76. https://doi.org/10.1146/annurev-clinpsy-032511-143049

Whitfield-Gabrieli, S., Thermenos, H. W., Milanovic, S., Tsuang, M. T., Faraone, S. V., McCarley, R. W., Shenton, M. E., Green, A. I., Nieto-Castanon, A., LaViolette, P., Wojcik, J., Gabrieli, J. D. E., & Seidman, L. J. (2009). Hyperactivity and hyperconnectivity of the default network in schizophrenia and in first-degree relatives of persons with schizophrenia. *Proceedings of the National Academy of Sciences*, *106*(4), 1279–1284. https://doi.org/10.1073/pnas.0809141106

Witter, M. P., & Amaral, D. G. (2021). The entorhinal cortex of the monkey: VI. Organization of projections from the hippocampus, subiculum, presubiculum, and parasubiculum. *Journal of Comparative Neurology*, *529*(4), 828–852. https://doi.org/10.1002/cne.24983

Witter, M. P., Hoesen, G. V., & Amaral, D. G. (1989). Topographical organization of the entorhinal projection to the dentate gyrus of the monkey. *Journal of Neuroscience*, *9*(1), 216–228. https://doi.org/10.1523/JNEUROSCI.09-01-00216.1989

Wu, J. W., Hussaini, S. A., Bastille, I. M., Rodriguez, G. A., Mrejeru, A., Rilett, K., Sanders, D. W., Cook, C., Fu, H., Boonen, R. A. C. M., Herman, M., Nahmani, E., Emrani, S., Figueroa, Y. H., Diamond, M. I., Clelland, C. L., Wray, S., & Duff, K. E. (2016). Neuronal activity enhances tau propagation and tau pathology in vivo. *Nature Neuroscience*, *19*(8), Article 8. https://doi.org/10.1038/nn.4328

Xie, L., Wisse, L. E. M., Das, S. R., Vergnet, N., Dong, M., Ittyerah, R., de Flores, R., Yushkevich, P. A., Wolk, D. A., & Initiative, for the A. D. N. (2020). Longitudinal atrophy in early Braak regions in preclinical Alzheimer's disease. *Human Brain Mapping*, *41*(16), 4704–4717. https://doi.org/10.1002/hbm.25151

Yarkoni, T., Poldrack, R. A., Nichols, T. E., Van Essen, D. C., & Wager, T. D. (2011). Large-scale automated synthesis of human functional neuroimaging data. *Nature Methods*, *8*(8), Article 8. https://doi.org/10.1038/nmeth.1635

Yassa, M. A., Muftuler, L. T., & Stark, C. E. L. (2010). Ultrahigh-resolution microstructural diffusion tensor imaging reveals perforant path degradation in aged humans in vivo. *Proceedings of the National Academy of Sciences*, *107*(28), 12687–12691. https://doi.org/10.1073/pnas.1002113107

Yeo, B. T., Krienen, F. M., Sepulcre, J., Sabuncu, M. R., Lashkari, D., Hollinshead, M., Roffman, J. L., Smoller, J. W., Zöllei, L., Polimeni, J. R., Fischl, B., Liu, H., & Buckner, R. L. (2011). The organization of the human cerebral cortex estimated by intrinsic functional connectivity. *Journal of Neurophysiology*, *106*(3), 1125–1165. https://doi.org/10.1152/jn.00338.2011

Zhang, J., Kucyi, A., Raya, J., Nielsen, A. N., Nomi, J. S., Damoiseaux, J. S., Greene, D. J., Horovitz, S. G., Uddin, L. Q., & Whitfield-Gabrieli, S. (2021). What have we really learned from functional connectivity in clinical populations? *NeuroImage*, *242*, 118466. https://doi.org/10.1016/j.neuroimage.2021.118466

Zhong, Q., Xu, H., Qin, J., Zeng, L.-L., Hu, D., & Shen, H. (2019). Functional parcellation of the hippocampus from resting-state dynamic functional connectivity. *Brain Research*, *1715*, 165–175. https://doi.org/10.1016/j.brainres.2019.03.023